PLASMA PROCESSES IN THE INNER COMA

T. E. CRAVENS
Department of Physics and Astronomy
The University of Kansas
Lawrence, KS 66045
U.S.A.

ABSTRACT. The solar wind interaction with comets is characterized by the mass-loading of the solar wind with heavy cometary ions that are produced by the ionization of neutrals in the extensive cometary coma. This mass-loading slows down the solar wind and ultimately leads to the formation of a magnetic barrier and a magnetotail. Solar wind protons disappear in the vicinity of the cometopause due to charge-exchange collisions with neutrals. The plasma and fields inside the cometopause of comets Halley and Giacobini-Zinner were observed by instruments on board several spacecraft. Several plasma populations were detected in the inner coma, including cold (less than 1 eV) and energetic (several keV or more) ions, and cold and hot electrons. The Giotto magnetometer observed a diamagnetic cavity surrounding the nucleus, which is a consequence of an outward ion-neutral drag associated with the flow of cometary neutrals past plasma frozen onto field lines in the magnetic barrier. In addition to large-scale structures, many small-scale structures in the plasma and fields have been observed in comets, including tail rays and kinks, and plasma pile-ups and depletions in the barrier. Theoretically, the existence of a very narrow layer of enhanced plasma density just inside the diamagnetic cavity boundary has been predicted. The behavior of plasma in the inner coma (within the cometopause) of an active comet is determined both by plasma processes, such as magnetohydrodynamics, and by collisional processes such as ion-neutral friction, resistivity, electron and ion thermal cooling, ion-neutral chemical reactions, and electron-ion recombination.

1. Introduction

Our understanding of cometary plasma processes has increased dramatically due to the data returned by the International Cometary Explorer (ICE) mission to comet Giacobini-Zinner (G-Z) and by the many missions to comet P/Halley such as VEGA, Giotto, and Suisei. Ground-based observations have also made a major contribution to cometary plasma physics, especially to an understanding of the ion tail. Several plasma populations were observed in the inner coma of comet Halley, including energetic cometary ions, cold cometary ions, solar wind electrons, and cold electrons. The plasma near active comets is a mixture of both solar wind and cometary plasma. The behavior of the plasma in the inner coma is determined by plasma processes such as magnetohydrodynamics (MHD) and by collisional processes such as ion-neutral friction, resistivity, electron and ion thermal cooling, and ion-neutral chemical reactions.

This paper will review the physical processes that determine the plasma behavior in the inner coma region of active comets, which is considered here to refer to the region inside the cometopause. The reader is also referred to other review papers. Some pre-Halley encounter reviews include those by Ip and Axford (1982) and Mendis *et al.* (1985). More recent reviews that include some Halley and G-Z encounter results were written by Galeev (1986) and Ip and Axford (1989) for cometary plasma processes in general, by Cravens (1987a) and Huebner (1989, this book) for the ionosphere, and by Cravens (1989a,b) for cometary plasma boundaries.

The contents of this paper are as follows:

2.   Overview of the Solar Wind Interaction With Comets and Ion Pick-Up

The interaction of the solar wind with a comet is collisionless at large cometocentric distances. The relatively slowly moving (typical outflow speeds of $v_g \approx 1$ km/s) cometary neutral molecules and atoms are "invisible" to the solar wind until such time as they are ionized. The newly created cometary ions accelerate in response to the interplanetary magnetic field ($\mathbf{B}$) and the motional electric field of the solar wind ($\mathbf{E} = -\mathbf{u} \times \mathbf{B}$, where $\mathbf{u}$ is the solar wind velocity). Section 2.1 reviews source and loss processes for cometary plasma.

2.1. SOURCES AND SINKS OF PLASMA

The main sources of ionization in rough order of importance are photoionization by solar extreme ultraviolet radiation, charge transfer of solar wind protons with cometary neutrals, and electron impact ionization (cf. Mendis *et al.*, 1985; Cravens *et al.*, 1987; Gombosi *et al.*, 1986). The following reactions illustrate these sources, where M stands for a cometary neutral species such as H_2O, CO, O, or H (see the chapters in this book by Huebner and see Krankowsky *et al.*, 1986):

$$h\nu \; + \; M \; \text{------>} \; M^+ \; + \; e \tag{1}$$

$$H^+ \; + \; M \; \text{------>} \; H_{fast} \; + \; M^+ \tag{2}$$

$$e \; + \; M \; \text{------>} \; M^+ \; + \; e + e \tag{3}$$

H^+ represents solar wind protons, in which case, reaction (2) produces cometary plasma. The H atoms resulting from reaction (2) are quite fast (speeds of about $u \approx 100$ km/s to 400 km/s). The photoionization rate at 1 AU is $I \approx 5 \times 10^{-7}$ s^{-1} for solar minimum solar conditions (cf. Korosmezey *et al.*, 1987), and the rates for the other processes are somewhat less than this, except perhaps for electron impact ionization in the presence of accelerated electrons in the inner coma (Cravens *et al.*, 1987; Schwingenschuh *et al.*, 1987).

The composition of cometary plasma can be altered in several ways. Charge transfer between ion species X^+ and neutral species M is represented by:

$$X^+ \; + \; M \; \text{------>} \; X \; + \; M^+ \tag{4}$$

X^+ can represent any cometary ion such as O^+, H_2O^+, or cometary H^+. Charge transfer of cometary pick-up ions also removes energy from the plasma, as well as modifying its composition, since ions picked up far upstream of the nucleus are quite energetic (i.e., they have energies of about 20 keV), whereas the replacement ions (M^+) are less energetic.

Cometary ions are produced millions of kilometers from the nucleus of active comets because their neutral comae are so extensive. The total neutral density is approximately given by:

$$n_n = \frac{Q_n}{4\pi v_g\, r^2} \exp[-r/\lambda]$$

(5)

where v_g is the neutral outflow speed (≈ 1 km/s), r is the cometocentric distance, $\lambda = v_g/I$ (≈ 1 to 2 million km) is the neutral attenuation length due to ionization, and $Q_n = 7 \times 10^{29}$ s^{-1} (for Halley) is the total cometary gas production rate.

The composition of cometary plasma can also be altered by ion-neutral chemical reactions other than charge-transfer, such as atom-atom interchange:

$$X^+ \quad + \quad YM \quad ------> XY^+ \quad + \quad M$$

(6)
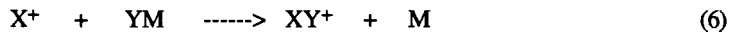
For example, for $X = H_2O$, $Y = H$ and $M = OH$, the following very important reaction is obtained:

$$H_2O^+ \quad + \quad H_2O \quad ------> H_3O^+ \quad + \quad OH$$

(7)
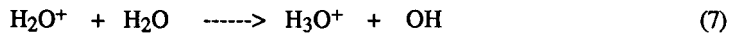
Reaction (7) has the consequence that the major ion in the inner comae of active comets is H_3O^+ rather than H_2O^+. The reaction rate coefficient for (7) is $k_{in} = 2.09 \times 10^{-9}$ cm^{3}s^{-1}, which is typical for this type of reaction (Mendis et al., 1985; Huebner, 1985; Huntress et al., 1986). Hundreds of these types of reactions are possible in the cold, partially ionized cometary plasma found in the inner coma (see the chapter by Huebner in this book).

Another chemical reaction, which is important in the inner coma and which neutralizes the plasma, is dissociative recombination:

$$XY^+ \quad + \quad e \quad ------> \quad X + Y$$

(8)

The most important example of this type of reaction is the dissociative recombination of H_3O^+.

$$H_3O^+ \quad + \quad e \quad ------> \quad H_2O + H$$

(9)
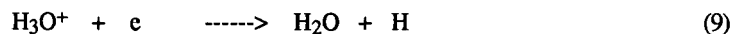
The reaction rate coefficient is $\alpha = 5 \times 10^{-7} (300/T_e)^{1/2}$ cm^{3}s^{-1} (see the chapter by Huebner for a more complete discussion of chemical reactions). Chemical reactions such as (4) - (9) are important only where the plasma is cold (T ≈ 1 eV) and dense, and where the neutral density is high -- that is, in the inner coma. On the other hand, the ion sources are important millions of kilometers upstream of the bow shock.

2.2. COMETARY ION PICK-UP BY THE SOLAR WIND

The ion pick-up process will be briefly reviewed here, because it has relevance even for the inner coma. A more complete treatment of the plasma physics of cometary ion pick-up can be found in

the chapter by Galeev in this book, and in several review papers (Ip and Axford, 1982; Galeev *et al.*, 1986; Lee, 1989; Terasawa, 1989).

A newly born cometary ion typically moves at the neutral speed of about 1 km/s in the cometary frame of reference, whereas the solar wind speed is about 400 km/s. The new cometary ion is initially almost at rest, but is subsequently accelerated by the motional electric field of the solar wind. The resulting ion trajectory, for almost uniform electric and magnetic fields, is cycloidal, with both gyromotion and $E \times B$ drift motion. The gyration speed is ($v_{perp} = u \sin \theta_{vB}$), where θ_{vB} is the angle between the solar wind velocity and the magnetic field. The resulting velocity-space distribution is a ring-beam distribution, with a parallel velocity (in the solar wind reference frame (SWRF)) of $u \cos \theta_{vB}$. This distribution is highly unstable to the formation of ultra-low frequency waves, and indeed, the measured magnetic field in the vicinity of the bow shocks of comets Giacobini-Zinner and Halley indicates the presence of very large amplitude ($\delta B/B \approx 1$) magnetic fluctuations. These fluctuations rapidly pitch-angle scatter ions from the ring in velocity space onto a spherical shell whose radius is u and whose center is at the solar wind velocity vector. Actually, the center of the shell would be shifted into the wave frame of reference if most of the waves travel in one direction along the magnetic field. Some ions are also accelerated by wave-particle interactions. The cometary bow shock can also energize ions.

The ion distribution function is affected by collisions in the inner coma, and ultimately, very close to the comet (cometocentric distances, r, within several thousand kilometers for an active comet like Halley), collisions enforce a Maxwellian distribution. The evolution of the cometary ion distribution function is shown schematically in Figure 1.

The SWRF energy of ions in a pick-up shell (neglecting stochastic acceleration) is $E = 1/2 \, m \, u^2$, which is typically about 20 keV for O^+ ions picked up far upstream of the shock. The solar wind slows down (or is "mass-loaded") as more and more cometary ions are added. Cometary ions born closer to the comet are picked up at smaller values of u, and, after being pitch-angle scattered, form a shell distribution with a smaller radius. The shells associated with ions picked up further upstream actually increase their radius slightly due to adiabatic compression. The solar wind speed drops relatively sharply at the bow shock, and thus ions picked up in the shocked solar wind are significantly less energetic than ions born upstream of the shock.
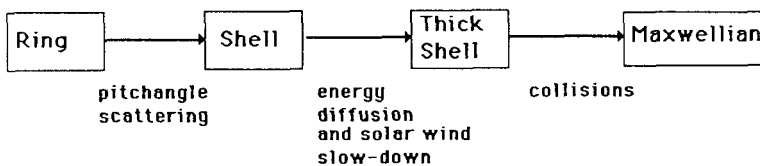

Figure. 1. Schematic of evolution of the distribution function of cometary pick-up ions as the comet is approached.

Figure 2 shows a cometary ion shell distribution function versus the energy calculated prior to the encounter for a cometocentric distance downstream of the bow shock (Galeev *et al.*, 1985). The distribution function has a high-energy (hot) component, formed upstream of the shock, and a low-energy (or cold) component formed downstream of the shock. Actual distributions are more diffuse than this calculated one, due to energy diffusion. But, overall, ions retain, in their energy, a memory of where they were born, and the SWRF energy of pick-up ions decreases with decreasing cometocentric distance. Actual distribution functions are quite complicated, especially near the bow shock, and are neither fully ring or shell (Neugebauer *et al.*, 1987; Neugebauer, 1990). Further details of the pick-up process are left to the Galeev chapter in this book.

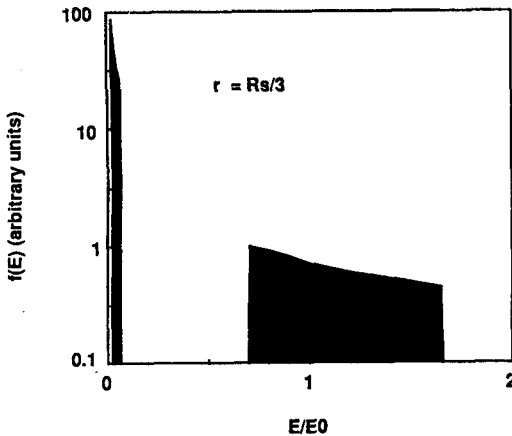## Cometary Ion Distribution Function

Figure 2. A theoretical cometary ion distribution function in the shocked solar wind is shown as a function of ion energy relative to the energy of a pick-up ion in the unperturbed solar wind far from the nucleus. Shell distributions in the solar wind reference frame were assumed and energy diffusion due to wave-particle interactions was neglected. This particular distribution is for a distance along the Sun-comet axis one third of the distance from the nucleus to the bow shock. From Galeev *et al.* (1985).

2.3. PLASMA DYNAMICS

The dynamics of the solar wind contaminated with cometary ions does not depend on the details of the particle distribution functions, but does depend on the overall pressure and density associated with the distribution functions.

The pressure for a species, j, with a shell distribution is given by:

$$p_j = \frac{1}{3} m_j \int_0^\infty \bar{v}^2 f_j(\bar{v}) 4\pi \bar{v}^2 d\bar{v}$$

(10)

where $f_j(v)$ is the distribution function of species j in the solar wind reference frame and $\bar{v}$ is the velocity in the solar wind reference frame. The sum of the pressures of all charged particle species gives the total pressure, $p = \Sigma \, p_j$. The "thermal" speed (i.e., the radius of the shell in velocity space) of cometary pick-up ions is on the order of the solar wind speed, and the pick-up ions are therefore quite hot (with SWRF energies of about 10 to 20 keV), whereas solar wind proton thermal energies are roughly 10 eV. Hence, the cometary ion component dominates the total pressure even at very large cometocentric distances. The pressure p increases with decreasing cometocentric distance, as more and more hot cometary ions are added to the solar wind flow.

A single fluid approach is very successful in describing most aspects of the solar wind flow near comets if the pressure of all important species is included (solar wind protons and electrons and cometary ions) and if mass addition due to ionization of cometary neutrals is included. However, more plasma components are needed to understand some phenomena such as the cometopause (Gombosi, 1987). The cometopause is a transition region found in the vicinity of 10^5 km (for comet Halley), where the plasma composition changes from primarily solar wind (protons and He^{++}) to primarily cometary (Gringauz et al., 1986a). A simple one-dimensional set of fluid equations is useful upstream of the cometary bow shock (Biermann et al., 1967; Wallis and Ong, 1974; Galeev et al., 1985; Galeev, 1986; Gombosi, 1987). The one-dimensional continuity equation is:

$$\frac{\partial}{\partial x}[\rho u] = I \frac{Q_n m_c}{4\pi v_g r^2} \exp[-r/\lambda]$$

(11)

ρ is the total mass density, ρu is the mass flux towards the comet, m_c is the mass of a typical cometary ion ($m_c \approx 16$ amu), and x is the distance along a solar wind streamline. Far upstream of the comet, $\rho u = n_{sw} m_p u$, where $n_{sw} \approx 5$ cm^{-3} is the solar wind number density and m_p is the proton mass. A somewhat different version of the one-dimensional continuity equation can be used downstream of the bow shock along the Sun-comet axis (Galeev et al., 1985):

$$\frac{1}{A}\frac{\partial}{\partial x}[A\rho u] = I \frac{Q_n m_c}{4\pi v_g r^2} \exp[-r/\lambda]$$

(12)

A(x) is the area of the flow tube as a function of distance along Sun-comet axis. The product, uA, is almost a constant along the Sun-comet axis.

The one-dimensional momentum equation far from the nucleus is given to a good approximation as:

$$\frac{\partial}{\partial x}\left[\rho u^2 + p + B^2/2\mu_0\right] = 0$$

(13)

where $B^2/2\mu_0$ is the magnetic pressure and p is the total pressure. The magnetic pressure gradient term is not very important upstream of the bow shock, and the solution to equation (13) is $\rho u^2 + p$ = constant.

The addition of cometary ions to the flow has two major effects as the comet is approached more closely: (1) The pressure increases with the addition of increasing numbers of hot cometary ions, and (2) the mass flux increases according to (11) or (12). Since both ρu and p increase, but $\rho u^2 + p$ must remain constant, the solar wind flow speed u decreases with decreasing cometocentric distance. In other words, mass-loading slows down the solar wind. The fluid equation solutions do not continuously go from supersonic to subsonic values; a weak bow shock forms at a critical level of mass-loading (Biermann et al., 1967; Galeev et al., 1985; Schmidt and Wegmann, 1982; Galeev and Lipatov, 1984; Omidi et al., 1986; Cravens, 1989a).

Well downstream of the shock, a region of rapidly decreasing flow velocity exists (Galeev et al., 1985; Gombosi, 1987). This "stagnation" region is associated with rapidly increasing mass density (due to the production of cometary ions) (Galeev et al., 1985). The stagnation region is related to the cometopause, as will be discussed later. The magnetic field strength increases as the

solar wind slows down ($uB_\perp$ = constant for the region upstream of the shock). The magnetic field strength builds up rapidly near the stagnation region, thus forming a magnetic barrier (Neubauer, 1987).

Global two- or three-dimensional, magnetohydrodynamic (MHD) models very successfully describe most aspects of solar wind flow near comets, although the details of particle distribution functions are not taken into account (Schmidt *et al.*, 1986; Schmidt-Voigt, 1989; Schwingenschuh *et al.*, 1987; Ogino *et al.*, 1988; Fedder *et al.*, 1986; Boice *et al.*, 1986). In particular, global MHD models were able to explain most features of the magnetic field variations observed near comet Halley by magnetometers on board both the Giotto spacecraft (Schmidt *et al.*, 1986; Schmidt-Voigt, 1989) and the VEGA spacecraft (Schwingenschuh *et al.*, 1987), as long as suitable interplanetary magnetic field (IMF) rotations were incorporated into the models to account for temporal variations in the IMF direction. See the chapter in this book by Neubauer for a detailed comparison of the MHD models and the Giotto magnetic field data. Some results of a MHD model of comet Halley from Ogino *et al.* (1988) are reproduced in Figure 3. The bow shock is evident in these results, as is the cometopause (or stagnation) region where the cometary density builds up rapidly. It is apparent that the magnetotail is associated with draping of field lines, due to the extreme slowdown of field lines inside the cometopause (or stagnation region).

3.   Plasma Populations in the Vicinity of Comets

Cometary ions picked up upstream of the bow shock are energetic ($\approx$ 10-20 keV in the SWRF for O^+), but ions picked up downstream of the shock are relatively cold. The plasma found in the inner coma of a comet is a mixture of many different plasma populations and includes not only the relatively cold cometary ions picked up locally, but also the much more energetic cometary ions picked up far upstream. A particular plasma population retains a memory of its birthplace via its SWRF energy (or "temperature"), although the details of its distribution function are altered by wave-particle interactions or by collisions in the inner coma.

Figure 4 is a schematic of the cometary plasma environment, showing where various plasma populations originate and where they typically terminate due to collisional processes (the ends of the arrows). Solar wind protons and electrons obviously originate upstream of the shock. Solar wind protons are removed from the flow near the cometopause by charge-exchange collisions with cometary neutrals, as will be discussed later. The distribution of solar wind (or magnetosheath) electrons is modified by collisions inside about 10^4 km (Gan and Cravens, 1990). Many species of energetic cometary ions are born upstream of the shock, including O^+, C^+, N^+, and cometary H^+ (ring and shell distributions). Downstream of the shock, the pick-up ions are colder ($E \approx 1$ keV -- warm ions) due to the slower flow speed and can be considered to be a distinct population (see Figure 2). The hot and warm cometary ions charge-exchange with neutrals near the cometopause and disappear from the plasma. Inside the cometopause, where the flow speed is very low, pick-up ions are cold, very abundant, and strongly modified by collisions (including chemistry).
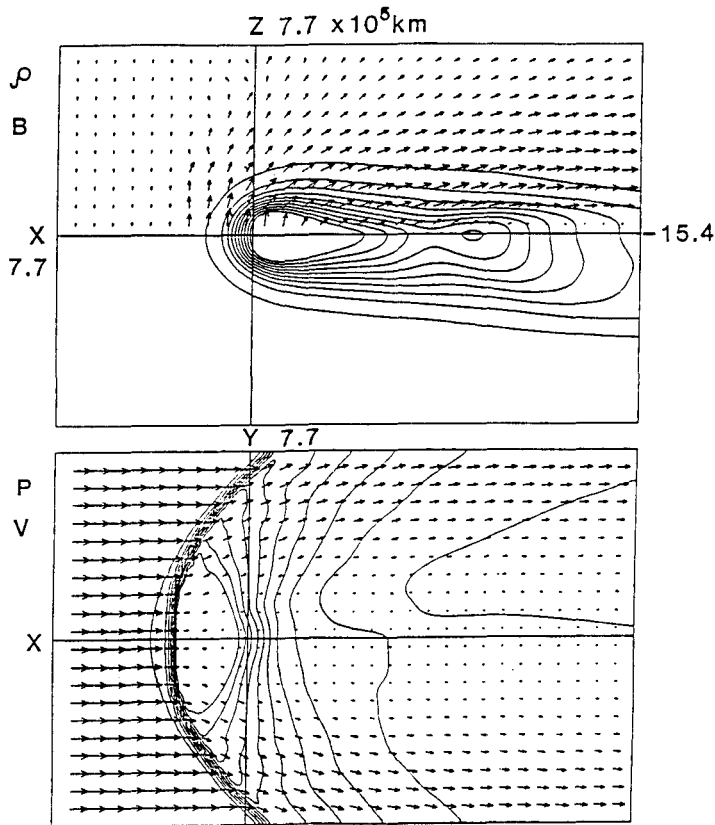
Figure 3. Results of a one-fluid global MHD model of comet Halley. The top panel shows magnetic field vectors and mass density contours, and the bottom panel shows solar wind velocity vectors and pressure contours. The bow shock, stagnation region (and magnetic barrier), and magnetotail are apparent. From Ogino *et al.* (1988).
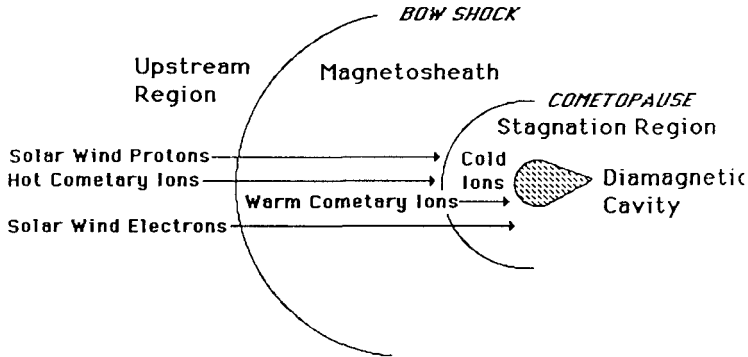
Figure 4. Schematic of the solar wind interaction with a comet, showing the origin of various plasma populations.

Table 1 provides a summary of the plasma populations found near the cometopause and their characteristics. Of course, this summary is oversimplified. For example, entirely separate hot (20 keV) and warm (1 keV) ion populations do not exist -- the distributions merge together more continuously; but the distinction is still useful. Figure 5 shows a cometary ion distribution function measured by the plasma analyzer on the Suisei spacecraft when it was somewhat outside the cometopause at $r = 1.8 \times 10^5$ km (Mukai *et al.*, 1986a,b). Clearly, the distribution is shell-like with a shell radius (i.e., "thermal" speed) in velocity space about equal to the flow speed at that location ($u \approx 80$ km/s).

Photoelectrons (also listed in Table 1) originate from the photoionization of cometary neutrals by solar extreme ultraviolet radiation. Photoelectrons are produced wherever neutrals are photoionized but are most abundant in the inner coma where the neutral density (and consequently the ion production rate) is the largest. Cold electrons are found only in the inner coma, since collisional cooling is required for their formation from the more energetic photoelectrons. Neutrals were also included in the table, although they are obviously not part of the plasma. The more energetic neutrals are created from the plasma by collisional processes such as dissociative recombination of cometary ions and charge-transfer of ions with other neutrals. These energetic neutrals can then be re-ionized and form a new plasma population (e.g., Eviatar *et al.*, 1989).

4.   Collisional and Transport Processes

4.1. THE COLLISIONOPAUSE

The plasma well outside the cometopause is largely collisionless, but collision processes become increasing important with decreasing cometocentric distance, as both the neutral and ionized gases become increasingly dense and as the bulk flow speed decreases. The collisionopause can be defined as the location, or boundary, at which collisions first become important (Marconi and

TABLE 1. Plasma Populations Found in the Vicinity of Comets

| Population	Type of Distribution	Temperature/Energy
PROTONS		
Solar Wind	Maxwellian	2 eV (but 1-keV total energy)
Cometary/Hot	Ring-Shell	1 keV
Cometary/Warm	Shell	100 eV
HEAVY COMETARY IONS		
Hot	Ring-Shell	20 keV
Warm	Shell	1 keV
Cold	Maxwellian	$\approx$1 eV
ELECTRONS		
Solar Wind/Magnetosheath	Maxwellian	10 to 30 eV
Photoelectrons	Non-Maxwellian	20 eV
Cold/Cometary	Maxwellian	$\approx$1 eV
Accelerated Electrons (?)	Beam	Several keV
COMETARY NEUTRALS		
Cold	$v \approx 1$ km/s	100 K
Warm (Dissociative Recombination, Charge Transfer)	$v \approx 1$ to 30 km/s	
Very Warm (Charge Transfer With Warm Ions)	$v \approx 30$ to 100 km/s	
Hot (Charge Transfer With Hot Ions)	$v \approx 400$ km/s	
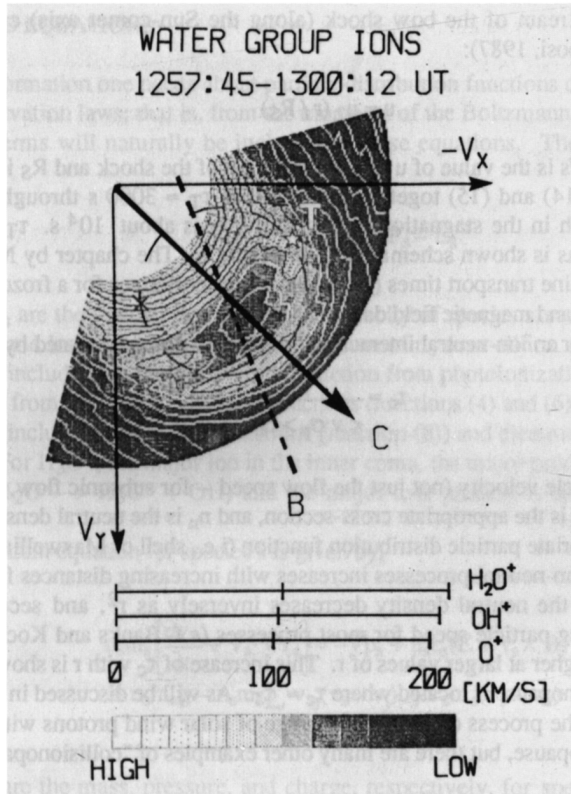
Figure 5. Velocity space distribution of cometary ions measured at a distance of 1.8×10^5 km from the comet Halley nucleus by the electrostatic analyzer on the Suisei spacecraft. The distribution is largely shell-like. The dashed line labeled B indicates the magnetic field direction, and the line C should be ignored. From Mukai *et al.* (1989).

Mendis, 1986; Houpis, 1988). There are many kinds of collisional processes, such as charge-transfer, electron cooling, and ion-neutral chemistry, and the collisionopause for each process will located at a different cometocentric distance (Cravens, 1989a).

The location of the collisionopause can be estimated by determining where the characteristic transport time (τ_T) for a process becomes comparable to the characteristic collision time (τ_C). The transport time is the residence time of the plasma within the region of interest and is approximately given by the ratio of the cometocentric distance and the flow speed at that location:

$$\tau_T \approx r/u \tag{14}$$

The flow speed downstream of the bow shock (along the Sun-comet axis) can be expressed approximately as (Gombosi, 1987):

$$u = u_2 \, (r / R_S) \tag{15}$$

where $u_2 \approx 100\text{-}150$ km/s is the value of u just downstream of the shock and R_S is the position of the shock. Equations (14) and (15) together indicate that $\tau_T \approx 3000$ s throughout most of the magnetosheath, although in the stagnation region itself, τ_T is about 10^4 s. τ_T increases with decreasing values of r, as is shown schematically in Figure 6. The chapter by Neubauer (in this volume) discusses field line transport times (i.e., plasma transport times for a frozen-in field) in the context of MHD models and magnetic field data.

The collision time for an ion-neutral interaction process, p, can be estimated by:

$$\tau_c \approx \frac{1}{<v \, \sigma_p> n_n} \tag{16}$$

where v is the total particle velocity (not just the flow speed -- for subsonic flow, v is about equal to the thermal speed), σ_p is the appropriate cross-section, and n_n is the neutral density. The average is taken using the appropriate particle distribution function (i.e., shell or Maxwellian, depending on the conditions). τ_c for ion-neutral processes increases with increasing distances from the nucleus for two reasons. First, the neutral density decreases inversely as r^2, and second, σ_p usually decreases with increasing particle speed for most processes (c.f. Banks and Kockarts, 1973) and the particle speeds are higher at larger values of r. This increase of τ_c with r is shown schematically in Figure 6. The collisionopause is located where $\tau_c \approx \tau_T$. As will be discussed in the next section, the collisionopause for the process of charge-exchange of solar wind protons with neutrals is the same thing as the cometopause, but there are many other examples of "collisionopauses."
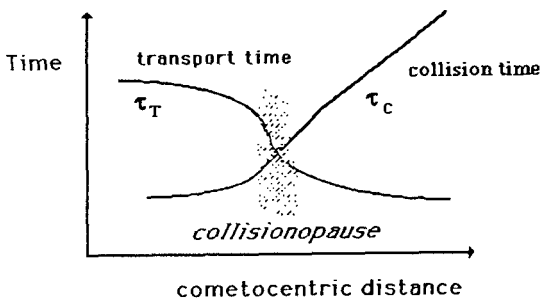

Figure 6. Schematic showing transport and collision time constants.

4.2. THE FLUID EQUATIONS

Most of the information one needs about particle distribution functions can usually be determined from the conservation laws; that is, from the moments of the Boltzmann equation. Both transport and collision terms will naturally be included in these equations. The continuity equation for species s is:

$$\frac{\partial n_s}{\partial t} + \nabla \cdot (n_s v_s) = P_s - L_s \tag{17}$$

where n_s and v_s are the number density and the velocity of species s, respectively. P_s and L_s are the production and loss rates, respectively. The sum of n_s over all ion species yields the electron density, n_e. P_s includes not only primary production from photoionization (reactions (1)-(3)), but also production from ion-neutral chemical reactions (reactions (4) and (6)). L_s includes all relevant loss processes, including ion-neutral reactions (reaction (6)) and electron-ion recombination (e.g., reaction (8)). For H_3O^+, the major ion in the inner coma, the major production process is reaction (7) $(H_2O^+ + H_2O ---> H_3O^+ + OH)$ and the major loss process is dissociative recombination (reaction (9)).

The momentum equation for species s is given by:

$$n_s m_s \left[\frac{\partial v_s}{\partial t} + v_s \cdot \nabla v_s \right] = -\nabla p_s + n_s e_s (E + v_s \times B)$$
$$+ n_s m_s g - n_s m_s \sum_j v_{sj}(v_s - v_j) + P_s m_s (v_s - v_n) \tag{18}$$

m_s, p_s, and e_s are the mass, pressure, and charge, respectively, for species s. v_n is the neutral velocity, which is usually quite small in comparison with the plasma velocity. E and B are the electric and magnetic fields, respectively. $g = -g \hat{z}$ is the acceleration due to gravity, which is negligible for comets, and v_{sj} is the effective momentum transfer collision frequency between species s and j (Banks and Kockarts, 1973). The pressure is given by equation (10), but can be written as an equation of state: $p_s = n_s k_B T_s$, where k_B is Boltzmann's constant and T_s is the temperature of species s. Temperature must be interpreted carefully for a non-Maxwellian plasma. The terms in equation (18) are mostly self-explanatory: from the left, we have the inertial and advection terms, the pressure gradient force term, the Lorentz force term, the gravitational term, the friction (or collision) term, and the mass-loading term.

Many possible simplifications can be made to equation (18). If the momentum equations for all species, including electrons, are added together, the electric field term disappears and one obtains the single fluid momentum equation for the bulk (center of mass) flow velocity u:

$$\rho \left(\frac{\partial u}{\partial t} + u \cdot \nabla u \right) = J \times B - \nabla(p_e + p_i) + \rho g - \rho v_{in}(u - v_n) \tag{19}$$

$\rho = m_i n_e$ is the mass density of the plasma and v_{in} is the ion-neutral momentum transfer collision frequency. The electron and total ion pressures (p_e and p_i, respectively) are included separately. Using Ampére's law, $\nabla \times B = \mu_0 J$, the $J \times B$ term can be expressed in terms of a magnetic

curvature force, $\mathbf{B} \cdot \nabla \mathbf{B} / \mu_0$, and a gradient of magnetic pressure, $-\nabla(B^2/2\mu_0)$, where the magnetic pressure is $p_B = B^2/2\mu_0$. $\mathbf{J}$ is the current density. A simplified 1-D form of this equation was shown in the last section. This simplification is justified outside the inner coma, but inside the "collisionopause for dynamics," both the $\mathbf{J} \times \mathbf{B}$ term and the ion-neutral friction term must be included.

Energy equations are also required for the electrons and ions, and can be quite complicated for non-Maxwellian distributions, but standard versions can be used for the Maxwellian plasma in the inner coma. Further discussion of electron and ion energetics in the inner coma will be given in a later section.

An equation for the magnetic field can be obtained from Faraday's law: $\partial \mathbf{B}/\partial t = -\nabla \times \mathbf{E}$. The electric field for a quasi-neutral plasma can be found from the electron momentum equation (i.e., the generalized Ohm's law -- see Siscoe, 1983). A simple form of this equation, which neglects the electron inertial terms and the Hall term, is:

$$\mathbf{E} = -\mathbf{u} \times \mathbf{B} + \eta \, \mathbf{J} \tag{20}$$

where η is the electrical resistivity of the plasma, which is proportional to the total electron collision frequency (cf. Siscoe, 1983).

Faraday's law, Ampere's law, and equation (20) put together yield the magnetic convection-diffusion equation that is standard in MHD theory:

$$\frac{\partial \mathbf{B}}{\partial t} = \nabla \times (\mathbf{u} \times \mathbf{B}) - \nabla \times (D \, \nabla \times \mathbf{B}) \tag{21}$$

where $D = \eta / \mu_0$ is the magnetic diffusion coefficient. The first term on the right-hand side of equation (21) accounts for the convection of magnetic flux with the plasma. The second term on the right-hand side of equation (21) represents the effects of the Ohmic dissipation of the electrical currents responsible for the magnetic field; this term is zero in a collisionless plasma, in which case the magnetic field is said to be "frozen-in." For comets, the magnetic diffusion term can be neglected everywhere, except in the immediate vicinity of the diamagnetic cavity boundary (Cravens, 1989b; Buti and Eviatar, 1989; also see the chapter by Neubauer in this book). The set of equations just discussed here, together with energy equations, constitute the MHD equations for the plasma, and provide a good description for most, although not all, plasma processes in the inner coma. A more detailed application of sections 2, 3, and 4 to various regions of the inner coma will be given in the remainder of this chapter.

5.   The Cometopause

5.1. OBSERVATIONS

Downstream of the bow shock, the solar wind flow continues to slow down (Balsiger, 1989; Mukai et al., 1986a; Schwenn et al., 1986) and becomes very slow, or stagnant (few km/s), for cometocentric distances less than 10^5 km. The magnetic field builds up rapidly in this region, forming a magnetic barrier (Neubauer, 1986, 1987; Riedler et al., 1986). As discussed earlier, global MHD models describe rather well the large-scale dynamics of the plasma flow downstream

of the shock, including the stagnation region and the magnetotail, but measurements made by instruments on several spacecraft have shown that the structure of the stagnation region is rather complicated. Gringauz *et al.* (1986a,b) (using data from the PLASMAG instruments on the VEGA 1 and 2 spacecraft) reported that a sharp "chemical" transition, which was called the cometopause, existed near the stagnation region of comet Halley, across which the plasma composition changed from primarily solar wind to primarily cometary.

A compositional transition region was also seen in the Giotto ion mass spectrometer (IMS) data; both solar wind protons and He^{++} densities dropped off from $r = 2 \times 10^5$ km to $r = 1 \times 10^5$ km, and the densities of various cometary species increased in this region (Balsiger, 1989). Figure 7 shows Giotto IMS data from both the low-energy (HIS) and high-energy (HERS) spectrometers for the vicinity of the cometopause. The HERS spectrometer measures O^+ ions of intermediate energy; this population of O^+ ions was picked up by the flow downstream of the shock but upstream of the stagnation region. This population disappears at about 80,000 km (closer to the nucleus than the proton fall-off distance), just as a new, colder, population of O^+ ions (measured by the HIS spectrometer) makes its appearance. Also measured by the HIS spectrometer, but not shown in this particular figure, are many other species of relatively cold and dense cometary ions, such as H_2O^+, OH^+, and CO^+ ions. H_3O^+ is shown, but is discussed in the next section. The cometopause seen by the Giotto IMS was much more gradual than the "sharp" cometopause seen by the VEGA plasma detector, but the apparent sharpness might be due to the instrumental observing geometry (Galeev *et al.*, 1988). According to the Giotto observations, a sharp transition region does not exist, and thus the term "cometopause" is somewhat misleading. However, this term is now being widely used, although it generally refers to a broad transition region across which the plasma composition changes from solar wind to cometary.

The flux of very energetic cometary ions, picked up by the solar wind upstream of the bow shock, was also observed to decrease in the general vicinity of the cometopause (Somogyi *et al.*, 1986; McKenna-Lawlor *et al.*, 1986; Kirsch *et al.*, 1987). Figure 8 shows data from three energy channels of the TUNDE energetic particle telescope on VEGA-1 for a time period encompassing the closest approach to the nucleus (Somogyi *et al.*, 1986). Fewer energetic ions were present for cometocentric distances within 1×10^5 to 2×10^5 km, except for the region right near closest approach, which will be addressed later.

5.2. THEORY

Several theoretical studies have been made of the cometopause region. Prior to the recent spacecraft-comet encounters, the semi-kinetic method was used to model the stagnation region (Galeev *et al.*, 1985; Wallis and Ong, 1975). Shell distribution functions were assumed to exist downstream of the shock, and both hot and cold cometary ion populations were postulated to exist (Figure 2). The hot population was predicted to contribute most of the pressure, and it was also suggested (Galeev *et al.*, 1985; Wallis and Ong, 1975) that the hot ions would undergo charge-exchange collisions in the vicinity of the stagnation region, thus cooling the plasma and delaying the complete stagnation of the flow.

Gombosi (1987) generalized these theoretical ideas, and included solar wind protons that charge-exchange with neutrals near the cometopause. He carefully evaluated the various collision terms in the 2-fluid (solar wind protons and cometary ions, but a common flow speed was assumed) conservation relations, assuming spherical shell distribution functions. He solved these equations along the Sun-comet axis with the assumption that the shocked subsonic flow is incompressible, such that $u(x)A(x) = $ constant, where $A(x)$ is the cross-sectional area of the flow
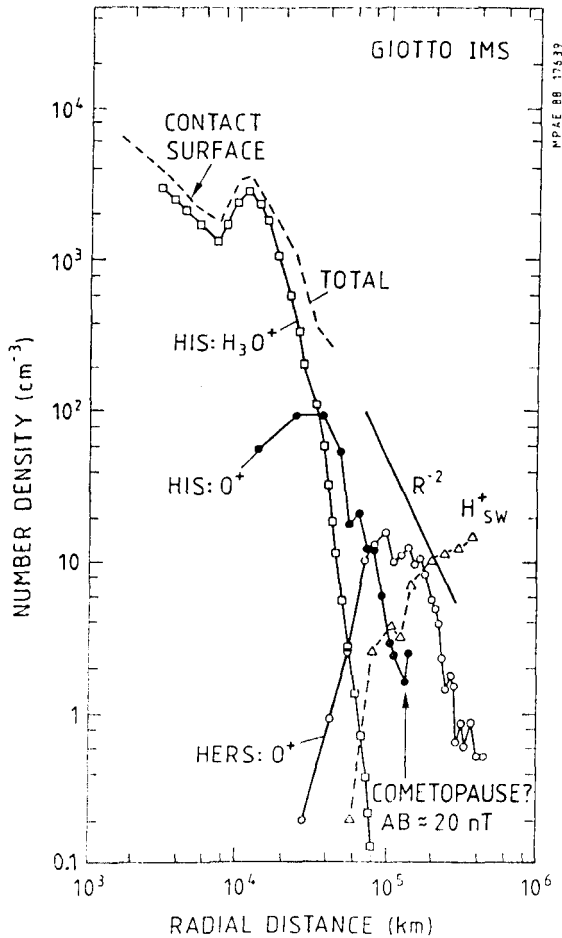
Figure 7. Number density versus cometocentric distance at comet Halley for several ion species from the HIS and HERS sensors on the Giotto ion mass spectrometer (Balsiger *et al.*, 1986,; Balsiger, 1989; Shelley *et al.*, 1987). From Ip and Axford (1989).
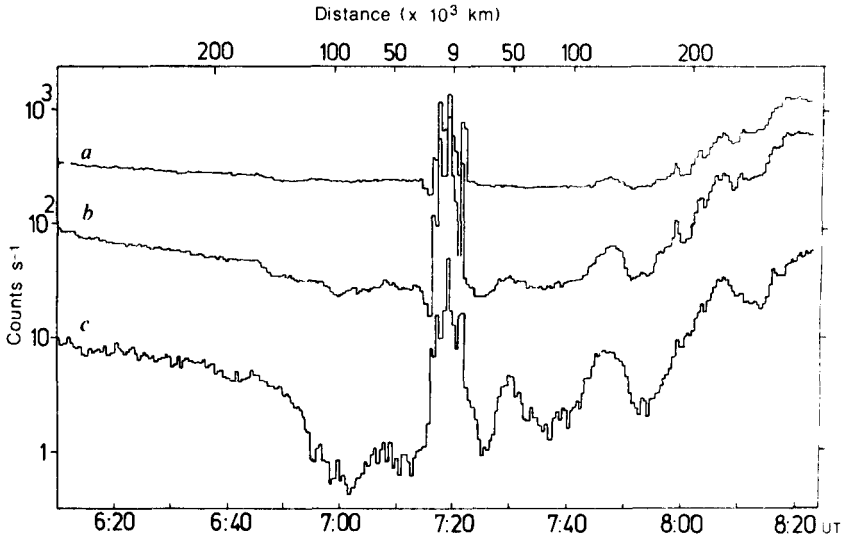
Figure 8. Counting rate (ion flux) versus time measured by the TUNDE energetic particle telescope during the VEGA-1 encounter with comet Halley. Results from three energy channels are shown: (a) 96 to 106 keV; (b) 106-126 keV; (c) 138-153 keV. From Somogyi *et al.* (1986).

tube defined by the streamlines. Calculated profiles of number density, flow speed, pressure, and temperature are shown in Figure 9 for comet Halley conditions. The solar wind density, n_{sw}, is roughly constant downstream of the bow shock until $r \approx 75,000$ km, where it decreases rapidly due to charge-exchange. The cometary ion density increases with decreasing r and, where its profile crosses that of n_{sw} near 75,000 km, is defined as the cometopause location, R_{com}. The pressures of both cometary ions and solar wind protons drop off rapidly near R_{com} as charge-exchange removes relatively hot ions and replaces them with colder, local pick-up ions. The flow speed decreases gradually throughout this region, varying in an almost linear manner with r (equation (15)).

Sauer *et al.* (1989) used a one-dimensional, multi-fluid, MHD model to investigate the plasma behavior in a region starting upstream of the shock and continuing down to the cometopause. Solar wind protons and cometary ions were each permitted to have independent flow velocities. A slowdown of the flow near 10^5 km was found, near where the flow first became sub-Alfvenic. However, the solution of the fluid equations was non-stationary in this region, which might explain some of the small-scale structure in the actual plasma data (e.g., Reme *et al.*, 1986). This model cannot yet be used to fully interpret the cometopause region, since charge-exchange reactions were omitted.

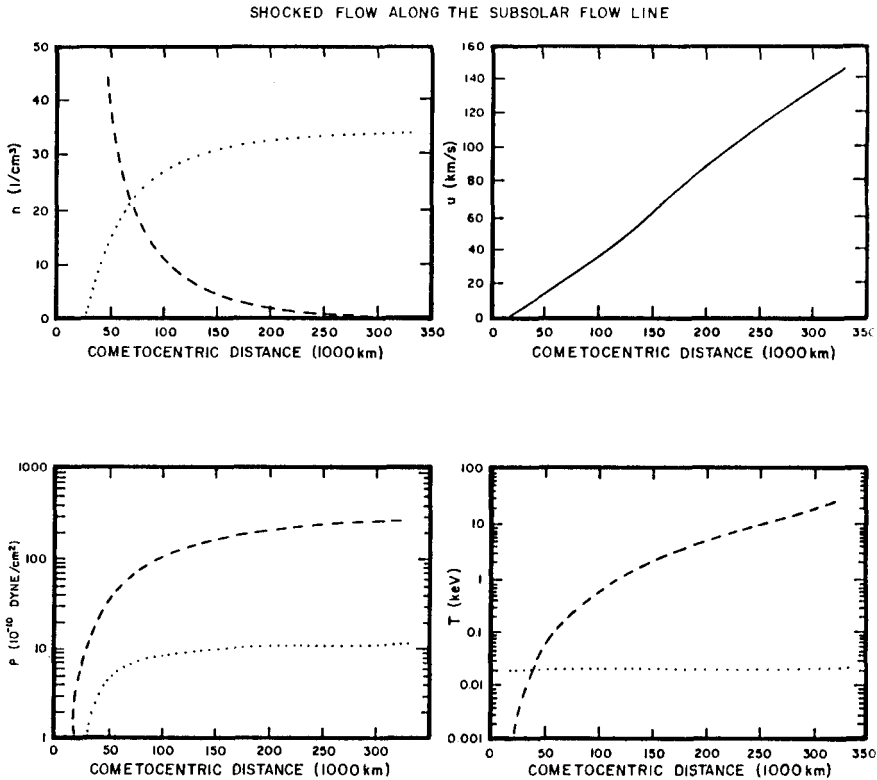SHOCKED FLOW ALONG THE SUBSOLAR FLOW LINE

Figure 9. Theoretically calculated profiles of plasma parameters versus radial distance in the vicinity of the cometopause. Upper left: Proton (dotted line) and cometary (dashed) number densities (cm^{-3}). Upper right: Flow speed (km/s) along the Sun-comet axis. Lower left: Proton (dotted line) and cometary (dashed) pressures (10^{-10} dynes/cm^2). Lower right: Proton (dotted) and cometary (dashed) temperatures (keV). From Gombosi (1987).

An analytic formula was derived by Gombosi (1987) which gives the cometocentric distance of the cometopause:

$$R_{com} = [R_0 \, r_1]^{1/2} \tag{22}$$

where R_0 is the classic collisionopause distance (Marconi and Mendis, 1986):

$$R_0 = \frac{\sigma_{cts}Q_n}{4\pi v_g}$$

(23)

Equation (23) can be derived by equating the collision mean free path for charge-transfer with the cometocentric distance, and then solving the resulting equation for r. $R_0 \approx 2 \times 10^4$ km for comet Halley parameters. $r_1 = 1.6 \times 10^5$ km is a characteristic length for the dynamics, defined as where the proton Mach number is equal to $[8/\pi g]^{1/2}$, with g being the ratio of specific heats. From (22), one finds $R_{com} = 6 \times 10^4$ km, which is much greater than R_0.

The cometopause can also be interpreted using the collisionopause concept discussed in section 4 (also see Cravens, 1989a). R_{com} is located where the charge-exchange time for solar wind protons is equal to their transport time (equation (15)). The appropriate speed in the collision time formula (equation (16)) is the proton thermal speed u_{th}, in which case, the following equation can be found:

$$R_{com} = \sqrt{\frac{u_{th}}{u_2} R_s R_0}$$

(24)

Cravens (1989a) found a value of $R_{com} \approx 1.5 \times 10^5$ km, by using a value of $u_{th} \approx u_{sw}$. However, this value of u_{th} is more appropriate for energetic cometary pick-up ions than it is for solar wind protons. With a more appropriate proton thermal speed of $u_{th} \approx 60$ km/s (Gombosi, 1987), equation (24) gives $R_{com} = 6 \times 10^4$ km, in agreement with the Gombosi value. R_{com} is much larger than R_0 because the protons gyrate about the field many times as they convect with the flow, thus increasing the probability of a collision.

The cometopauses observed both by Giotto (Balsiger, 1989) and VEGA (Gringauz et al., 1986b) were located at about 1.5×10^5 km (but the transition region is very broad for Giotto), rather than at the theoretical value of 6×10^4 km. Gombosi (1987) attributed this discrepancy to two-dimensional effects, because the data were obtained off to the sides and the theory was applicable to the Sun-comet axis. A different approach was taken by Ip (1989), in order to help resolve this discrepancy. Ion distributions as functions of thermal speed were found by solving continuity equations for several ion species (such as solar wind protons, O^+, OH^+, H_2O^+, and H_3O^+) along flow streamlines taken from the 3-D MHD model of comet Halley by J. Fedder. The dynamics were thus not included self-consistently, but 2-D effects were incorporated. Ip (1989) found that the cometopause was still only at 6×10^5 to 8×10^5 km for the Giotto trajectory and concluded that some physical processes might still be missing, such as ion species not having the same flow speed, which could lead to plasma instabilities such as the firehose instability (Galeev et al., 1988). The multi-fluid model of Sauer et al. might be very useful if charge-exchange were included. In fact, the VEGA-2 plasma measurements indicate that the solar wind proton and alpha particle speeds can differ by as much as 140 kilometers/second near the cometopause, and the difference for Giotto was tens of kilometers/second (cf. Fuselier et al., 1988; Formisano et al., 1988).

6. The Inner Coma

Now consider the behavior of the plasma and fields in the inner coma region -- defined as the region inside of the cometopause. Collisional processes become more important and more complicated than merely charge-transfer reactions. The more energetic ions begin to disappear and

are replaced by many species of colder ions. This section will contain several subsections, encompassing the measurements, photochemistry, the formation of the diamagnetic cavity, the structure of the cavity, plasma energetics, energetic ions and neutrals, and waves.

6.1. PLASMA AND FIELD MEASUREMENTS

For many years prior to the spacecraft encounters with comets Halley and Giacobini-Zinner, relatively cold "ionospheric" plasma has been postulated to exist in the inner comae of active comets (see the pre-encounter reviews by Mendis *et al.*, 1985; Ip and Axford, 1982; and Mendis and Houpis, 1982). The first direct evidence for the existence of this plasma was obtained by the Giotto, VEGA, and ICE spacecraft during their recent encounters with the above comets (see reviews by Cravens, 1986, and Ip and Axford, 1989). The first measurements of magnetic fields in the inner coma of comet Halley were made by the magnetometers on the VEGA and Giotto spacecraft (Riedler *et al.*, 1986; Neubauer *et al.*, 1986). The magnetic profile near the time of closest approach of Giotto to the nucleus is shown in Figure 10 (Wu, 1987). The theoretical profiles indicated in Figure 10 will be discussed later. The field strength is large in the stagnation region (i.e., the magnetic barrier), reaching a maximum of $B \approx 60$ nT at $r \approx 10^4$ km. The Giotto spacecraft encountered a diamagnetic cavity deep within the stagnation region (Neubauer *et al.*, 1986). The boundary of this field-free cavity will be called the diamagnetic cavity boundary surface (abbreviated CS), but it has also been called the contact surface, the ionopause, and the tangential discontinuity. The CS was crossed on the inbound leg of Giotto at a distance from the nucleus of $r_{cs} = 4470$ km, and the cavity was exited on the outbound leg at $r_{cs} = 4155$ km (Neubauer *et al.*, 1986).
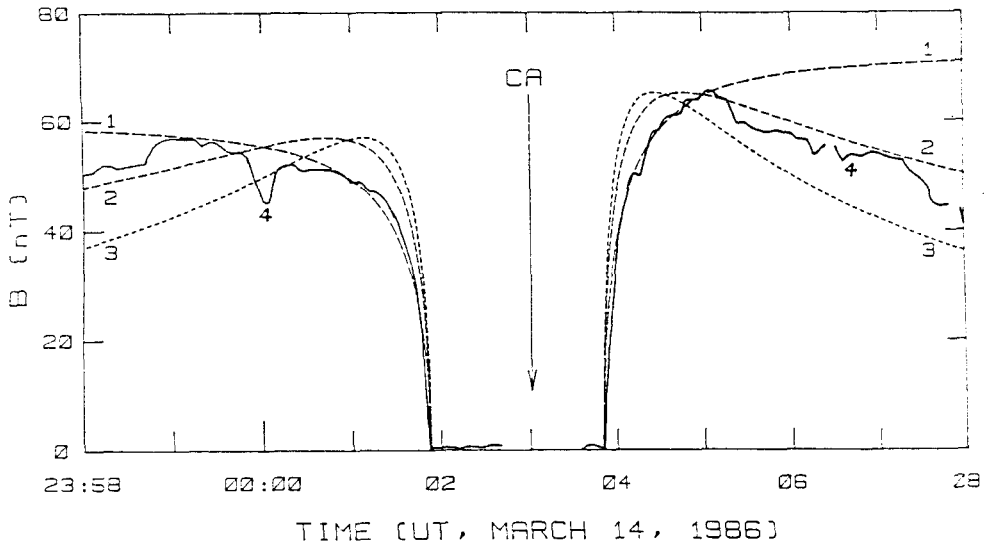

Figure 10. Theoretical (curve 1 from either Cravens (1986) or Wu (1987) and curves 2 and 3 from Ip and Axford (1987)) and measured (curve 4 from Neubauer *et al.* (1986)) magnetic field profiles for comet Halley. The diameter of the cavity is about 10^4 km. CA is the closest approach of the Giotto spacecraft to the nucleus. From Wu (1987).

The plasma in the inner coma of comet Halley (within $r \approx 10^5$ km) was observed to be almost stationary (u less than several km/s) and entirely of cometary origin (Gringauz *et al.*, 1986a,b; Balsiger *et al.*, 1986). Basic characteristics of the thermal plasma in the inner coma are evident in the data from the Giotto HIS ion mass spectrometer shown in Figures 7 and 11 (Balsiger *et al.*, 1986; Balsiger, 1989; Shelley *et al.*, 1987; Schwenn *et al.*, 1987). The radial component of the flow speed (shown in the top panel of Figure 11) is about equal to 1 km/s inside the diamagnetic cavity, which is equal to the neutral outflow speed (that is, $v_r \approx v_g$). v_r drops sharply at the CS, outside of which it remains less than 1 km/s out to $r \approx 20,000$ km. Everywhere within a distance of 4×10^4 km, the radial plasma flow speed remains less than a few kilometers/second (i.e., the plasma is stagnated). The non-radial flow speed was not directly measured but can be deduced from the ion temperature (Cravens, 1987b), as discussed in the next section; this component of the flow velocity is greater than v_r, but is still less than a few kilometers/second in this region. The densities of most ion species, including H_3O^+, were observed to be enhanced for cometocentric distances near 1×10^4 to 1.5×10^4 km. This has been called the "plasma pile-up."
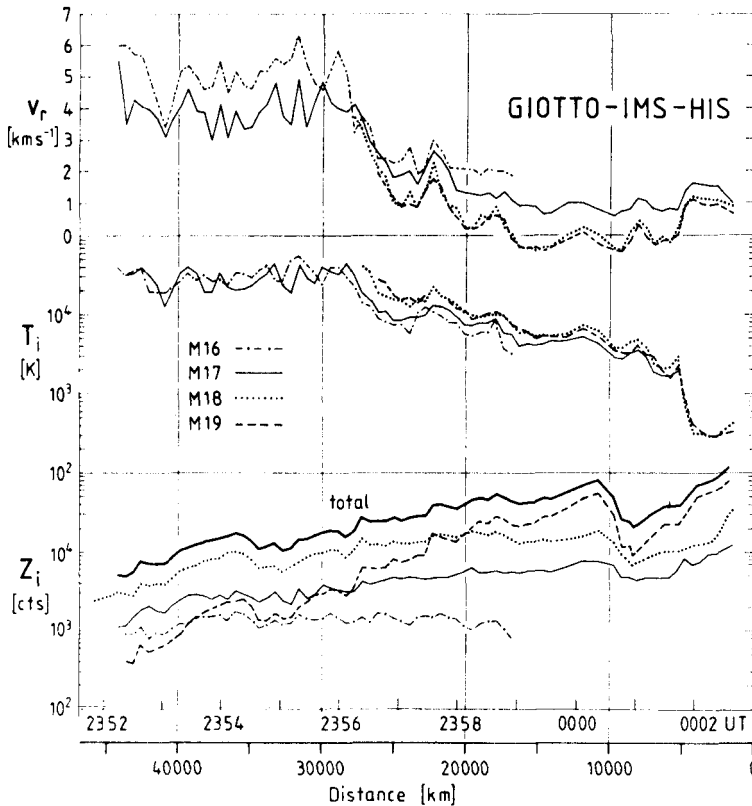

Figure 11. Plasma parameters in the inner coma of comet Halley measured by the Giotto ion mass spectrometer. Top panel: Ion velocity component along the Giotto trajectory (i.e., almost radial). Middle panel: Ion temperatures. Bottom panel: Ion densities (dividing the count rates by a factor of 10 roughly gives number densities in cm^{-3}). From Schwenn *et al.* (1987).

The ion temperature (Figure 11) is on the order of 10^3 to 10^4 K in the stagnation region, and drops sharply at the CS to values of ≈ 200 to 300 K. It should be noted that energetic, non-thermal, and low-density particle populations also exist in the inner coma, as well as the cold thermal plasma.

6.2. PHOTOCHEMISTRY AND THE CHEMICAL COLLISIONOPAUSE

Photochemistry including ion-neutral reactions and recombination starts to become important inside the cometopause (Mendis et al., 1985; Schmidt et al., 1988; Allen et al., 1987; and see Huebner's chapter). Inside the collisionopause for a particular species, photochemical processes dominate, and the net production rate is almost equal to zero: $P_s = L_s$.

Consider the H_2O^+ ion. These ions are primarily produced by photoionization of water with a production rate of $P_{H2O+} = I\, n_n$. The main loss process is reaction with water molecules (equation 7), giving a loss rate of $L_{H2O+} = k\, n_n\, n_{H2O+}$, where n_{H2O+} is the H_2O^+ number density. Inside the collisionopause, photochemical equilibrium applies and the local net production is approximately zero: $P_{H2O+} - L_{H2O+} = 0$. The solution of this equation is: $n_{H2O+} = I/k \approx 500$ cm^{-3}, independent of r. The counting rate for the mass 18 channel in the Giotto IMS profile is roughly constant (Schwenn et al., 1986), although inside $r \approx 2000$ km, NH_4^+ that is produced by reaction of H_3O^+ with ammonia also contributes to the signal in the mass 18 channel, according to Allen et al. (1987), thus causing a decrease of the mass 18 (H_2O^+ plus NH_4) density with r. Marconi and Mendis (1988) explain this density decrease without the relatively high ammonia abundance assumed by Allen et al. (1987).

The production rate of H_3O^+, assuming that it is the major ion (Aikin, 1974) with a density equal to n_e, is equal to $I n_n$ (all H_2O^+ production is assumed to go to H_3O^+ via reaction 7). The loss rate of H_3O^+ is given by $\alpha\, n_e^2$ (dissociative recombination, reaction 7). The photochemical expression for the electron density then can written as (Mendis et al., 1985; Cravens, 1987a; Cravens, 1989b):

$$n_e = \left[\frac{I\,Q_n}{4\pi\, v_g 7 \times 10^{-7}} \right]^{1/2} \left[\frac{T_e}{300} \right]^{1/4} \frac{1}{r} \tag{25}$$

A value of $n_e \approx 3000$ cm^{-3} near the CS of comet Halley ($r \approx 4500$ km) is obtained using equation (25) for an electron temperature of $T_e = 1000$ K. The electron temperature in the inner coma will be discussed in section 6.5.2 of this paper. It has long been recognized that the electron density in the cometary ionosphere should vary inversely with r (cf. Mendis et al., 1985; Ip and Axford, 1982). The Giotto IMS results have verified this (Balsiger et al.,1986; Schwenn et al., 1987; Figure 11). The total ion density was observed to vary as 1/r, more or less, out to $r \approx 10^4$ km. In fact, there was no significant deviation from this inverse r variation even at the CS; the density on both sides of the cavity boundary is photochemical. Thus, the CS is not an ionopause of the type found at Venus, where the ion density does indeed "pause" and the ionosphere disappears (cf. Brace et al., 1980).

The collisionopause for H_2O^+ can be found (Cravens, 1989a) by equating the transport time, $\tau_T \approx 10^4$ s, with the chemical lifetime, $\tau_c \approx 1/k\, n_n$:

$$R_{H2O+} \approx \sqrt{\frac{k\,Q_n\,\tau_T}{4\pi v_g}} \approx 40{,}000\ \text{km} \tag{26}$$

H_2O^+ ions are transport-controlled outside this distance, and the density decreases with r more rapidly than the photochemical expression indicates. The IMS data does show a change in the water ion profile near $r \approx 4 \times 10^4$ km. Similarly, comparing the relevant collision and transport times for the major ion, one finds that the collisionopause for H_3O^+ ions is located somewhere between 1×10^4 and 4×10^4 km.

Telescopic observations of H_2O^+ intensity (i.e., column density) profiles by Konno (1989) and Ip et al. (1986) show breaks at cometocentric distances of about 20,000 km for comet Halley and 1000 km for comet Giacobini-Zinner. These breaks can be interpreted as the H_2O^+ collisionopause. τ_T for Halley is ≈ 10 times larger than at G-Z, and Q_n is about 20 times greater. Equation (26) predicts, then, that the collisionopause at G-Z is located a factor of 20 closer to the nucleus than at Halley, in general agreement with the remote observations.

The enhancement of the H_3O^+ density near 10^4 km could be a signature of the collisionopause for that species, although similar enhancements are also evident for other species. The most likely explanations for this enhancement region are (Ip et al., 1987; Ip and Axford, 1989; Cravens, 1989b): (1) reduced ion loss associated with an elevated electron temperature at this location, (2) dynamical pile-up, (3) excess ionization, possibly due to electron impact, (4) a time-dependent phenomenon associated with changes in solar wind conditions or in the cometary outgassing rate. None of these explanations is entirely satisfactory (see the above references), although the first explanation seems to be the most plausible. The dissociative recombination coefficient decreases with increasing values of T_e, and thus an increase in the electron temperature leads to a decrease in the electron density according to equation (25).

6.3. FORMATION OF THE DIAMAGNETIC CAVITY

The formation of the diamagnetic cavity has been intensively studied since 1986 (Cravens, 1989b; Schmidt et al., 1986; Neubauer et al., 1986; Cravens, 1987a,b; Haerendel, 1987; Houpis, 1988; Cravens, 1986; Ip and Axford, 1987; Eviatar and Goldstein, 1989; Wu, 1987; Haerendel, 1986; Sauer and Baumgartel, 1986; Neubauer, 1986; Goldstein et al., 1989; Ershkovich et al., 1989). Both collisional and transport processes must be included in order to model the magnetic field in the stagnation region outside the diamagnetic cavity. In particular, both the $J \times B$ and the ion-neutral frictional force terms must be retained in the momentum equation (eq. 11).

6.3.1. Momentum Balance - Analytical Results.
Shortly after the Giotto encounter, both Ip and Axford (1987) and Cravens (1986, 1987a) recognized that the existence of the diamagnetic cavity is a consequence of the balance between an outward ion-neutral frictional force (due to the flow of neutrals past stagnated ions) and an inward-directed magnetic $J \times B$ force. The mass-loading term also plays a role, albeit secondary (Haerendel, 1987). The $J \times B$ force can be separated into a magnetic pressure gradient force and a curvature force. Figure 12 is a schematic of the force balance in the inner coma.

Analytical expressions for the field strength, B(r), have been obtained by several workers by integrating simplified forms of the momentum equation (19). Figure 10 includes several theoretical profiles. The profile labeled #1 (Wu, 1987; Cravens 1986, 1989c) was found by neglecting the curvature force, whereas for profiles 2 and 3 (Ip and Axford, 1987) the curvature force was included. Profile 1 agrees best of all the theoretical profiles with the data for the inbound leg, at least in the immediate vicinity of the CS, suggesting that the field lines are rather flat on the sides of the cavity. However, the measured outbound profile was obtained when Giotto was more towards the sunward direction than the inbound profile and agrees somewhat better with the theoretical

profiles calculated with curvature included.

The expression for profile 1 is (Cravens, 1986, 1989b):

$$B(r) = B_0 \sqrt{1 - \left[\frac{r_{cs}}{r}\right]^2}$$

(27)

where the distance to the cavity surface is given by:

$$r_{cs} = \left[\frac{I\, m_e^2\, k_{in}^2}{4\pi\, v_g\, \alpha}\right]^{1/4} \frac{Q_n^{3/4}}{B_0}$$

(28)

The momentum transfer collision frequency can be written as $v_{in} = k_{in}\, n_n$, where $k_{in} = 1 \times 10^{-9}$ $cm^3 s^{-1}$. B_0 is the field strength in the magnetic barrier. The magnetic field in the barrier can be estimated by equating the magnetic pressure $[B_0^2/2\mu_0]$ with the solar wind dynamic pressure. Equation (28) demonstrates that the cavity is larger for more active comets (larger gas production rate, Q_n) and smaller for larger B_0 (that is, for higher solar wind dynamic pressure conditions).

Global MHD models (Schmidt *et al.*, 1986) have indicated that the diamagnetic cavity is probably tear-drop shaped and elongated in the direction of the tail. Wu (1987) also demonstrated this from an analysis of the momentum balance.
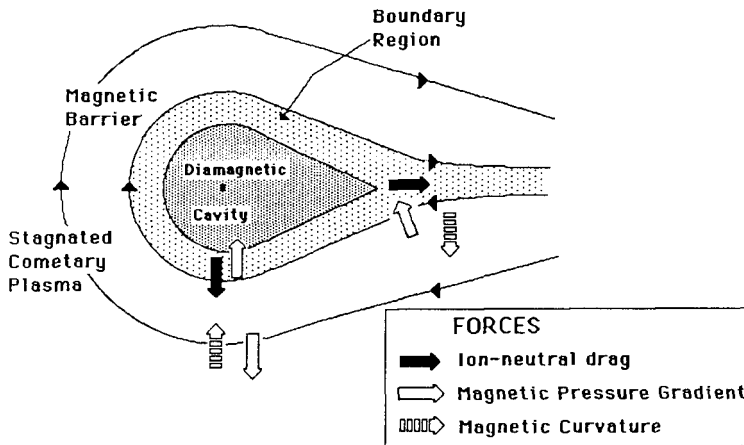

Figure 12. Schematic of the inner coma and diamagnetic cavity of comet Halley illustrating important terms in the force balance relation. A plausible field line configuration is indicated. From Cravens (1986).

6.3.2. *Numerical Models.* Global MHD models describe very well the large-scale structure ($\Delta r \approx 10^3$ km or more) of the cometary plasma environment, including the inner coma (Schmidt *et al.*, 1986; Ogino *et al.*, 1988; Fedder *et al.*, 1986; Boice *et al.*, 1986; Wegmann *et al.*, 1987). Other models have been developed to study the inner coma on smaller scales. Sauer and Baumgartel (1986) and Baumgartel and Sauer (1987) numerically solved one-dimensional, axisymmetric MHD equations along the Sun-comet axis for a variable cross-section flow tube. Ion-neutral friction and electron-ion recombination were included, and the grid size was 300 km. The results are shown in Figure 13. The calculated cavity boundary is located at 5000 km; the calculated plasma velocity is equal to v_g inside the diamagnetic cavity, is zero immediately outside the CS, and is 1 km/s (inward) further outside the CS. A small density enhancement ($\approx 30\%$) is present at the CS, suggesting that this boundary has some interesting structure (discussed in the next section).

Sauer and Baumgartel (1986) were able to obtain a significant density enhancement at a distance of 10^4 km (the "plasma pile-up") by sharply reducing the ion recombination rate at this distance. Cravens (1989b) constructed a high-resolution ($\Delta r \approx 4$ km near the CS), one-dimensional MHD model of the inner coma of comet Halley, and also obtained a density enhancement at the plasma pile-up region by increasing the electron temperature at 10^4 km.

6.4. STRUCTURE AND STABILITY OF THE CAVITY BOUNDARY SURFACE

6.4.1. *MHD Model of the Cavity Boundary Surface.* Cravens (1989b) used his high-resolution, one-dimensional MHD model to study the small-scale structure of the CS. Results from a preliminary version of this model were presented in 1987 (Cravens, 1987c). The one-fluid continuity, momentum, and energy equations for the major ion and the magnetic diffusion-convection equation were numerically solved, and an electron temperature profile was adopted. The momentum equation included a viscosity term. Results are shown in Figure 14.

Inside the diamagnetic cavity, the plasma and the neutral gas move together, and outside the cavity the plasma is stagnated. The transition between the two regions takes place over a 50-km-wide transition layer (the "cavity transition layer"). The transition is more rapid when the viscosity is lower; both of the viscosity values used in the numerical model are reasonable, given the uncertainties. The magnetic field profile is especially steep in the transition layer and the plasma density is enhanced by a factor of three. The ion temperature increases in two stages: first, from 300 to 600 K in the inner part of the layer, and then up to 800 K in the outer part of the layer.

The behavior of the plasma near the CS can be understood in terms of simple gas dynamic concepts. Ion-neutral friction can be neglected in the narrow confines of the layer (but not elsewhere), and thus from equation (13), the total pressure, including dynamic pressure, $\rho u^2 + p + B^2/2\mu_0$, is conserved across the layer. B is small in the inner part of the layer and $u = v_g$. As u decreases to zero, the thermal pressure p (and the density) must increase in order to keep the total pressure constant. Cravens (1989b) used this type of analysis to find a density enhancement of about 2.5, which was not too far from the numerical value. In the outer part of the layer, as the density (and pressure p) decreases due to excess electron-ion recombination, the magnetic pressure must increase in order to keep the total pressure constant. Once the magnitude of the density enhancement is known, one can estimate the thickness of the layer, Δ, by requiring that all the plasma flowing from the cavity towards the CS be consumed by excess ion-neutral recombination in the transition layer:

$$\Delta = \frac{v_g}{\alpha\, n_0} \frac{1}{\left(\frac{n_1}{n_0}\right)^2 - 1}$$

(29)

where n_0 is the unperturbed density and n_1 is the density in the layer. A large density enhancement, n_1/n_0, implies a thin layer, because the recombination rate is high in this case.
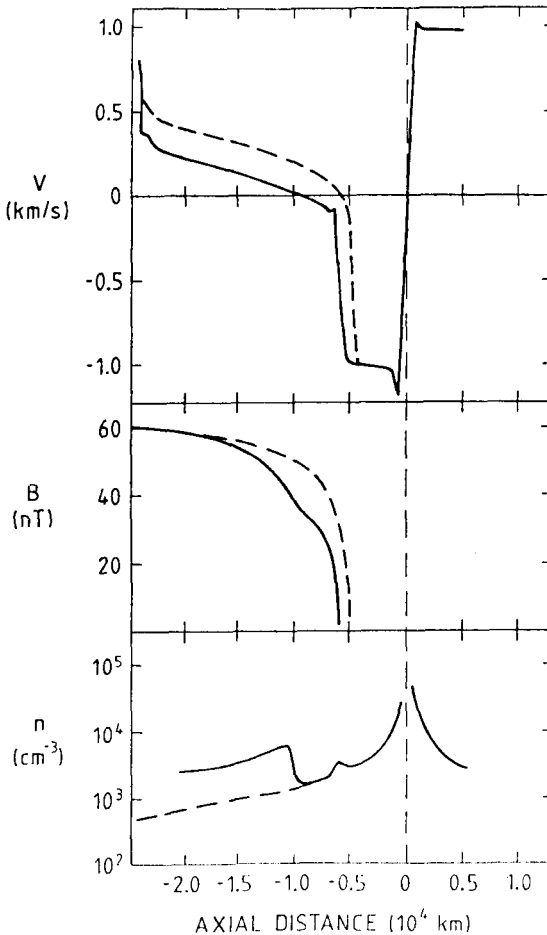

Figure 13. Profiles of plasma velocity, magnetic field strength, and plasma density versus distance along the Sun-comet axis from a one-dimensional MHD model. The solid lines are for a dissociative recombination coefficient $\alpha = 3 \times 10^{-7}$ cm^{3}s^{-1} for $r < 10^4$ km and $\alpha = 0$ for $r > 10^4$ km. The dashed lines are for $\alpha = 3 \times 10^{-7}$ cm^{3}s^{-1} everywhere. From Baumgartel and Sauer (1987).
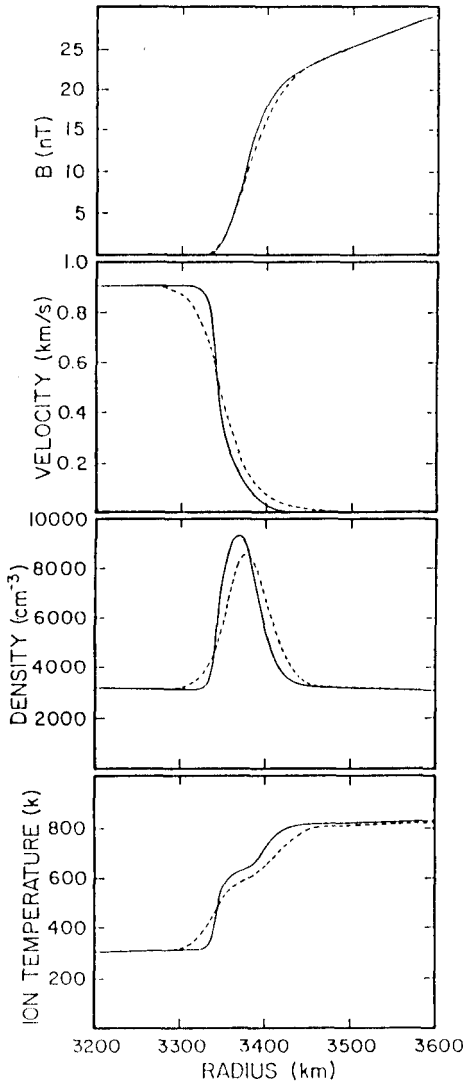
Figure 14. Profiles of magnetic field strength, plasma velocity (radial), plasma number density, and ion temperature versus cometocentric distance in the vicinity of the boundary surface of the comet Halley diamagnetic cavity, from a one-dimensional MHD model. The solid line is for low values of the viscosity and magnetic diffusion coefficient and the dashed line for higher values. From Cravens (1989b).

The inner parts of the density and velocity profiles appear to be steeper than the outer parts, and the ion temperature increases in two separate layers. Cravens (1989b) suggested that the first layer is the "inner shock," in which the incident supersonic flow (the sonic Mach number is 1.6) decelerates to subsonic values. The distance of this inner shock from the "obstacle" to the flow (the magnetic barrier) is about the same as the thickness of the shock itself. The inner shock, as originally conceived, was thought to be located a distance of about 1000 km from the diamagnetic cavity surface, and the flow was thought to encounter the shock and then be diverted tailward (Houpis and Mendis, 1980). However, Cravens (1989b) demonstrated that electron-ion recombination and ion-neutral friction require the shock to be located very near the obstacle.

A non-fluid interpretation of the transition layer is also possible (Ip and Axford, 1989). Ignoring collisions, an ion incident on the magnetic barrier from the inside will be reflected by the Lorentz force within about 20 km. The collision mean-free path is on the order of the thickness of the layer, so that neither the collisionless approach or the fluid approach can be strictly valid.

6.4.2. *Measurements of the Structure of the Cavity Surface*. Neubauer (1988) recently published a high-resolution magnetic field profile measured by the Giotto magnetometer (Figure 15). A 30-km-wide region of steep magnetic gradient is clearly evident at the CS. Neubauer (1988) suggested that this gradient could be explained without a density enhancement if the electron temperature inside and outside the cavity was about 10^4 K and 5000 K, respectively (thus creating a thermal pressure gradient). However, it is unlikely that the bulk of the electron population could have a temperature in excess of about 1000 K near the CS, due to strong electron-water cooling (Korosmezey *et al.*, 1987; Cravens and Korosmezey, 1986). However, superthermal electrons cannot be eliminated as a source of pressure. A magnetic perturbation was observed to be present at a distance of ≈ 150 km outside the CS, and was interpreted by Neubauer (1988) as an outwardly propagating magnetosonic pulse, created sometime earlier, perhaps by a flux of superthermal electrons generated in the tailward part of the cavity by reconnection.

The original analysis of the Giotto IMS data did not indicate the existence of a density enhancement at the CS, due to inadequate spatial resolution. The time required by the HIS spectrometer to obtain a full mass spectrum was 4 seconds, in which time the spacecraft traveled 300 km -- many times greater than the predicted thickness of the transition layer. However, several months ago, a special analysis of the data was performed, in which information obtained within an instrumental cycle was examined, and it now appears that a density enhancement between a factor of 3.5 and 20 is present at the CS (Goldstein *et al.*, 1989).

6.4.3. *Stability of the Cavity Boundary Surface*. Ip and Axford (1989) provide a good, concise review of this topic. The cavity surface must be basically stable because the cavity was observed to be field-free, although this does not exclude the possibility of waves along the surface itself. The boundary between the magnetized and unmagnetized regions was treated as a discontinuity prior to the encounters (e.g., Wallis and Dryer, 1976), in which case, this boundary is subject to the Kelvin-Helmholtz, as well as to Rayleigh-Taylor and fluting, instabilities (Ershkovich *et al.*, 1986; Ershkovich and Flammer, 1988). It was thus difficult to understand why this boundary is stable. However, the increase of the magnetic field is not present as a discontinuity, but as a broad region in which magnetic and frictional forces are in balance; this thickness plus the effects of photoionization and recombination tend to stabilize the boundary, or at least hold down wave growth rates to very low values.

6.5. ENERGETICS IN THE INNER COMA

6.5.1. *Ion Energetics*. Outside the cometopause, cometary ions are energetic and their distribution function is shell-like, rather than Maxwellian; but these hot ions are removed by charge-exchange and are replaced by colder ions picked up locally, as discussed in section 5. MHD simulations have demonstrated the transition from a predominantly hot ion population to a predominantly cold ion population. Figure 11 shows ion temperatures measured in the inner coma by the Giotto IMS.

Collisions become important in determining the nature of the distribution function, which should become Maxwellian; however, the transition from shell to Maxwellian has not been studied. In the collision-dominated region, the ion temperature can be determined theoretically by solving a standard energy equation (cf. Banks and Kockarts, 1973).
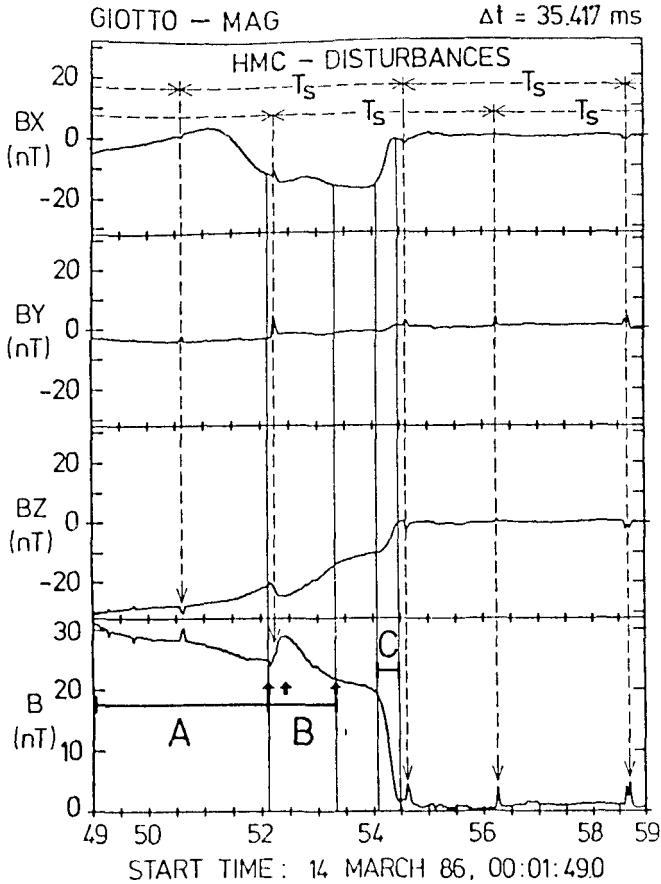
Figure 15. High-resolution magnetic field vector components (Halley-centered solar ecliptic coordinates) and total field strength measured on the inbound Giotto passage of the cavity surface (marked C). From Neubauer (1988).

In the inner coma, the ion energetics is determined by collisional processes such as photochemical heating, electron-ion energy transfer, ion-neutral frictional heating and ion-neutral cooling. Haerendel (1987) and Cravens (1987c) derived similar analytic formulae for the ion temperature, assuming local energy balance:

$$T_i = T_n + \Delta T_{chem} + \frac{m_c}{3k}|u - v_g|^2 \tag{30}$$

where T_n is the neutral temperature, k is Boltzmann's constant, and $\Delta T_{chem} \approx 100$ K (Cravens, 1987b) is the contribution to the ion temperature from photochemical heating. Inside the diamagnetic cavity, the ions and neutrals flow together, $u = v_g$, and the ion temperature is about equal to the neutral temperature ($T_i \approx 100$ to 300 K) as observed. The plasma stagnates just outside the CS ($u = 0$), and the last term in equation (30) contributes a temperature increase across the CS of about 800 K, in agreement with the measurements. The solution of the full energy equation, including heat conduction (which is not very important), was shown in Figure 14 (Cravens, 1989b); the increase of T_i across the CS is also affected by dynamical compression at the inner shock.

The measured ion temperature increases from 1000 K to about 10^4 K as r increases from 5000 km to about 2×10^4 km. This increase can be explained with equation (30) if the ion flow speeds are on the order of a few kilometers/second (Wegmann et al., 1987; Haerendel, 1987; Cravens, 1987b).

6.5.2. *Electron Energetics*. The electrons outside the inner coma are basically solar wind electrons, or shocked solar wind electrons (Reme et al., 1986; Gringauz et al., 1986a), but in the inner coma, collisions modify the solar wind electron distribution and photoionization generates photoelectrons (cf. Cravens et al., 1987). A transition region should exist somewhere inside the cometopause, in which solar wind electrons (both core and halo) and photoelectrons both exist in abundance. Cravens et al. (1987) called this region the plasma mantle, by analogy with a similar region outside the ionopause of Venus, in which the electron distribution was observed to have both solar wind and photoelectron components (Spenner et al., 1980). Electron distributions in the tail of comet Giacobini-Zinner (G-Z) were measured by the electron spectrometer on the ICE spacecraft (Bame et al., 1986; Zwickl et al., 1986). Zwickl et al. (1986) discerned three components: (1) a cold component with a density less than 10 cm^{-3} outside the plasmasheet, but with a much higher density inside, (2) a mid-component with $n_e \approx 20$ cm^{-3} and $T_e \approx 2 \times 10^5$ K, and (3) a hot component with $n_e \approx 0.3$ cm^{-3} and $T_e \approx 8 \times 10^5$ K. Zwickl et al. noted that the density of the mid-component is considerably greater than magnetosheath densities and suggested that photoelectrons from ionization of cometary neutrals contribute to this component.

Electron distributions in cometary ionospheres (as theoretically modeled by Mendis et al., 1985; Marconi and Mendis, 1986; Boice et al., 1986; Korosmezey et al., 1987; Gan and Cravens, 1990) are expected to have two major components: (1) a cold, dense population ($n_e \approx 10^3$ to 10^4 cm^{-3} and $T_e < 1$ to 2 eV), and (2) a more energetic photoelectron component whose energy spectrum has considerable structure due to the structure in the extreme ultraviolet spectrum of solar radiation (see Figure 16; Korosmezey et al., 1987; Gan and Cravens, 1990). The photoelectrons heat the colder thermal electrons via Coulomb collisions. All these calculations, except for those of Gan and Cravens (1990), are appropriate only for the unmagnetized ionosphere.
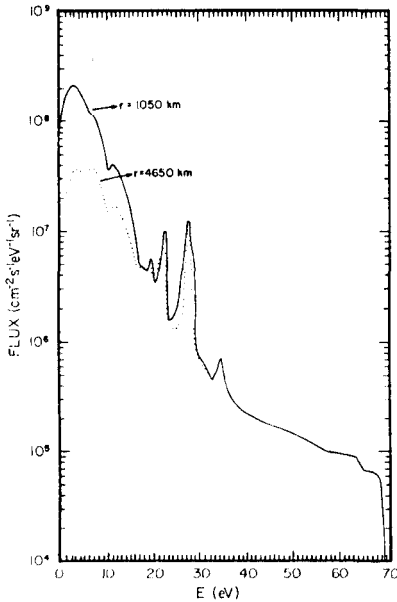
Figure 16. Theoretically calculated photo-electron fluxes versus energy for two cometocentric distances in the field-free iono-sphere of comet Halley. From Korosmezey *et al.* (1987).

The analysis of thermal noise detected by the radio experiment on the ICE spacecraft during its encounter with the near-tail region of G-Z clearly demonstrated (Meyer-Vernet *et al.*, 1986) the existence of ionospheric-type plasma in the narrow confines of the G-Z plasmasheet (see Figure 17--$n_e \approx 700$ cm^{-3} and $T_e \approx 1.4 \times 10^4$ K). The mid and hot electron components seen in the tail of G-Z by the ICE electron spectrometer were also present in the plasmasheet. The ionospheric models referenced above (e.g., Marconi and Mendis, 1986; Korosmezey *et al.*, 1987) indicate that the electron temperature within a few thousand kilometers of the nucleus is almost equal to the neutral temperature, due to cooling of the thermal electrons by rotational and vibrational excitation of water molecules (Cravens and Korosmezey, 1986). On the other hand, the Schmidt *et al.* (1988) MHD model generated electron temperatures as high as 10^4 K inside the cavity of comet Halley; however, thermal and photoelectrons were lumped together in that model. Ionospheric models indicate that T_e increases rapidly with r starting at some critical radial distance (which can be called the electron "thermal collisionopause"), due to thermal decoupling from the neutrals.

In the model of Gan and Cravens (1990), superthermal electrons (including both photoelectrons and solar wind electrons) were allowed to move along field lines, as well as to interact with the cold and cometary neutrals and thermal electrons. For the thermal electrons, the heat conduction equation was solved along field lines and included heating from Coulomb interactions between the cold and superthermal electrons and cooling due to electron-water collisions. Two regions are
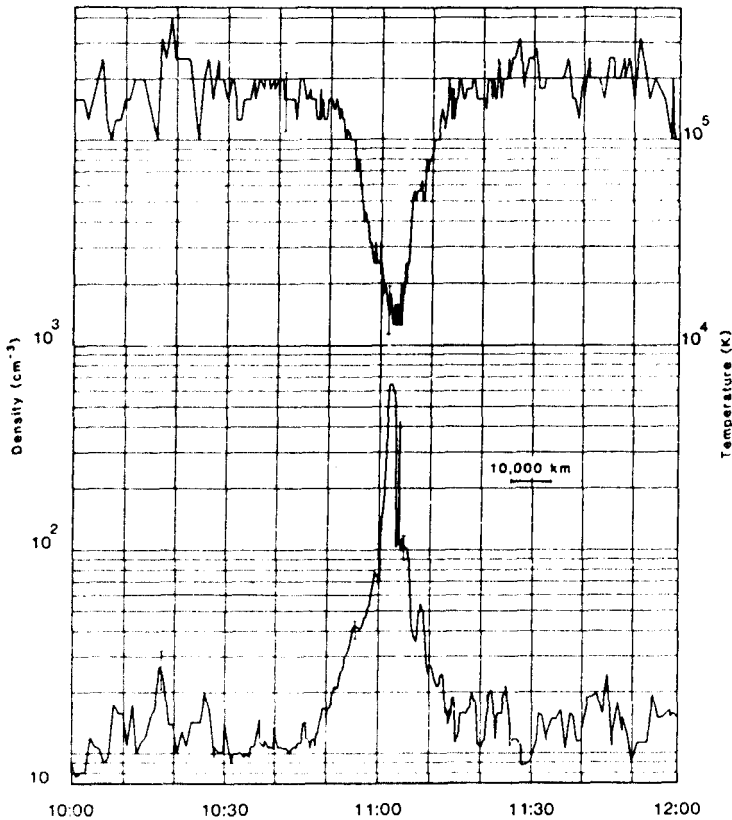
Figure 17. Electron density and temperature measured by the radio experiment on the ICE spacecraft during its traversal of the tail of comet Giacobini-Zinner. From Meyer-Vernet *et al.* (1986).

apparent in the results (Figure 18). The electron gas is very cold ($T_e < 1000$ K) in the inner region and is quite hot ($T_e > 10^4$ K) in the outer region. The transition region, or electron thermal collisionopause (Cravens, 1989b), is located at $r = 1.5 \times 10^4$ km in the subsolar region. The electron temperature is high outside this collisionopause, and continues to increase up to solar wind values ($T_e \approx 10^5$ K), although the Gan and Cravens model ceases to be valid for those conditions. The plasma density enhancement observed by the Giotto IMS near 1.5×10^4 km (Figure 9) might be partially explained by the presence of an electron temperature collisionopause, since the electron-ion dissociative recombination coefficient decreases with increasing T_e, as discussed earlier.
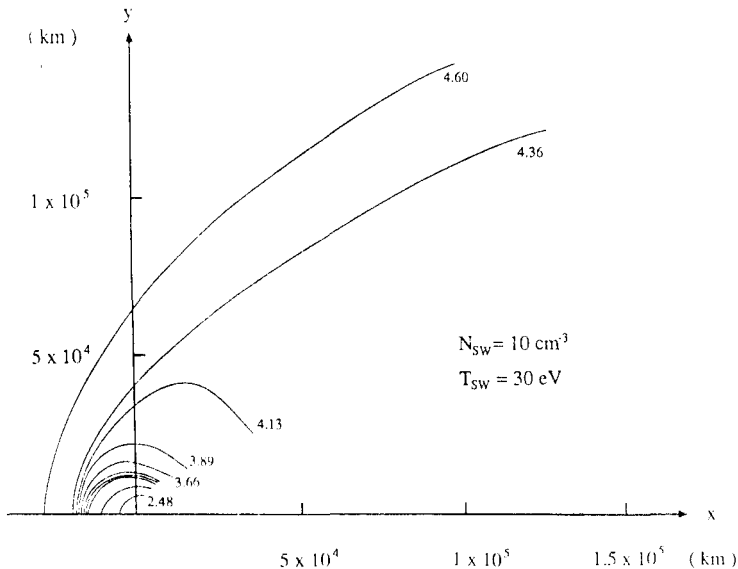
Figure 18. Theoretically calculated electron temperatures in the inner coma of comet Halley. Contours of $\log_{10}(T_e)$ are shown, as are the assumed solar wind (magnetosheath) conditions. The x-axis is along the Sun-comet axis. From Gan and Cravens (1990).

6.6. ENERGETIC IONS AND NEUTRALS IN THE INNER COMA

6.6.1. *Warm Ions and Neutrals.* The bulk of the plasma in the inner coma reflects the local flow conditions and is cold; however, more energetic superthermal populations are known to exist in the inner coma. Superthermal electrons have already been discussed. Hot and warm cometary ions, as well as solar wind protons, charge-exchange with cometary neutrals near the cometopause and disappear, as discussed in section 5. Giotto IMS data indicates that warm ions ($E \approx 100$ eV) make a reappearance inside the diamagnetic cavity (Johnstone *et al.*, 1986; Goldstein *et al.*, 1987). The following explanation for these ions has been offered (Eviatar and Goldstein, 1989). The fast neutrals ($v \approx 50$ km/s), which are produced well outside the cavity by the charge-transfer or dissociative recombination of warm ions picked up further upstream, get re-ionized as they traverse the cavity. The fresh ions are then scattered and observed by the IMS instrument. Ip (1989) used a Monte Carlo model to investigate the fast neutrals, and concluded that, although a significant population of energetic neutrals exists in the inner coma, the warm ions created by their re-ionization were not sufficiently abundant to account for the observations; however, work is actively continuing on this topic and this conclusion must be considered to be tentative. Ip suggested that magnetic re-connection in the tail might act as an additional source of warm ions.

6.6.2. *Energetic Ions and Neutrals.* Very energetic (E ≈ 100 keV) ions also experience charge-exchange collisions near the cometopause. The energetic heavy cometary ions fluxes measured by the TUNDE experiment on VEGA-1 decreased near the cometopause, but they made a "comeback" in the inner coma near 10^4 km (Figure 8). Similar measurements made by the Giotto EPONA experiment (Kirsch *et al.*, 1987) demonstrate that the flux of energetic cometary ions (and electrons) continues to increase with decreasing r inside the diamagnetic cavity (Figure 19), although the experimental difficulties in measuring energetic particles in the presence of dust impacts and gas particle impacts on the spacecraft close to the nucleus should be realized. Several explanations for these energetic ions have been offered, including entry of energetic pick-up ions into the cavity from the magnetosheath, Fermi acceleration of ions within the cavity, and field line merging on the front side of the cavity (Kirsch *et al.*, 1987; Verigin *et al.*, 1987). One difficulty with all these explanations is that the lifetime of a 100-keV O^+ ion against charge-transfer at r ≈ 3000 km is less than 5 s, which is insufficient for even a single transit of the cavity. The electron removal cross-section, which produces an ion from an energetic neutral, is about a factor of 10 smaller than the charge-transfer cross-section at these energies. Perhaps the very energetic neutrals from charge-transfer reactions at larger distances are being directly detected by the solid-state detectors on Giotto and VEGA-1. The dynamical effect of the pressure contributed by all these superthermal particle populations has not yet been assessed.
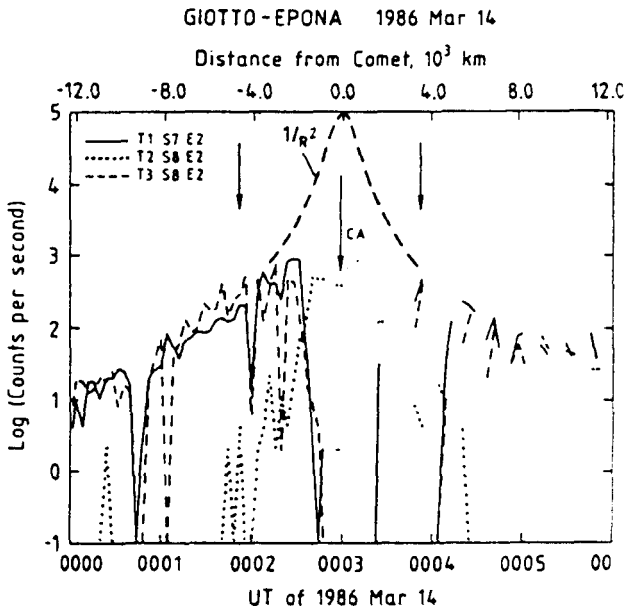

Figure 19. Energetic ion fluxes versus time in the inner coma of comet Halley, measured by the EPONA energetic particle telescopes on Giotto. Telescopes 1 and 3 measure in different directions, and channel 2 corresponds to 97- to 145-keV water group ions. Telescope 2 is foil-covered, and channel 2 corresponds to 30- to 60-keV electrons. The arrows indicate the cavity surface. From Kirsch *et al.* (1987).

6.7. PLASMA WAVES AND INSTABILITIES IN THE INNER COMA

Plasma waves play a pivotal role in the assimilation of newly picked-up cometary ions into the solar wind outside the inner coma (see the chapter on plasma waves in this book by Tsurutani), but collisional processes are more important than wave processes in the inner coma . The VEGA-1 and -2 spacecraft carried high-frequency plasma wave analyzers (APV-V) and measured a gradient in the electric field amplitude in the 8- to 14-Hz and 14- to 25-Hz channels near the cometopause (Grard *et al.*, 1987), interpreted as being due to lower-hybrid electrostatic plasma waves (Grard *et al.*, 1987; Mogilevsky *et al.*, 1987). Lower hybrid waves are produced by newly created pick-up ions and can transfer energy to superthermal electrons (cf. Galeev *et al.*, 1986; Ip and Axford, 1989).

The magnetometers on VEGA-1 and -2 observed waves in the inner coma (an example is shown in Figure 20 (from Russell, 1988)) that had the characteristics of the MHD slow mode, in which the magnetic field and plasma density variations are out of phase (Russell, 1988; Russell *et al.*, 1987). The suggested source of these waves was the mirror instability, and these waves might explain some of the small-scale structure observed in comets.

7. The Plasma Tail

A variety of structures have been remotely observed for many decades in cometary plasma tails (Brandt, 1982). A brief review is given here of plasma processes operating in the region of the tail relatively close to the inner coma. Comet tails are a consequence of the extreme mass-loading (and stagnation of the flow) that takes place ahead of the comet, and that results in the "draping" of the magnetic field lines. The ICE encounter with comet Giacobini-Zinner has provided the only *in*
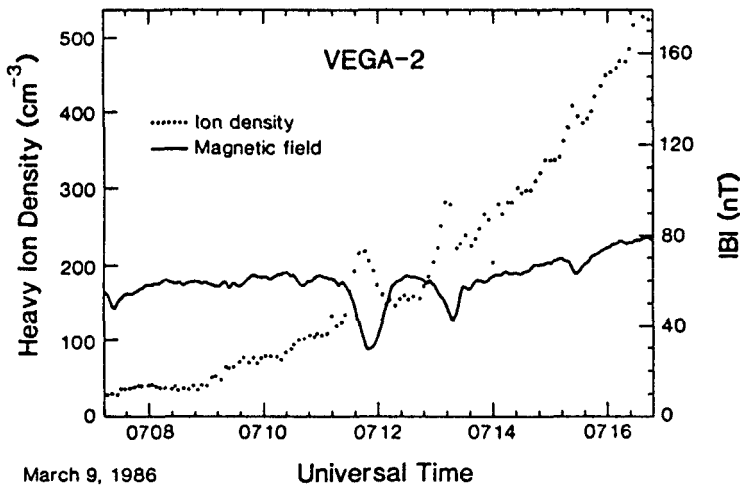

Figure 20. Ion density and magnetic field data measured in the stagnation region of comet Halley by instruments on VEGA-2. Ion condensation events caused perhaps by the mirror instability are evident. From Russell (1988).

situ measurements of a cometary plasma tail. A narrow layer of cold, dense plasma was observed in the middle of the tail (Meyer-Vernet *et al.*, 1986), as described in section 6 (Figure 17). Clear evidence for magnetic field line draping was obtained by the ICE magnetometer (Slavin *et al.*, 1986a,b).

The basic structural features of the cometary plasma tail, as learned from the ICE observations, were represented in a schematic (Figure 21) by Slavin *et al.* (1986c). A narrow plasmasheet, or neutral sheet (where the field strength is small and where the field has no component along the Sun-comet axis), is bounded by magnetotail lobes, where the field strength is high. The magnetosheath plasma is found outside the tail lobes (and magnetotail in general).

Two- and three-dimensional, global MHD models (e.g. Schmidt-Voigt, 1988, and references cited earlier) successfully reproduce the gross structure of cometary plasma tails, and even simple MHD concepts are conceptually very useful (Siscoe *et al.*, 1986; Ershkovich, 1981). The momentum equation, (13) or (19), takes the form of the following standard static pressure relation for the direction orthogonal to the tail axis:
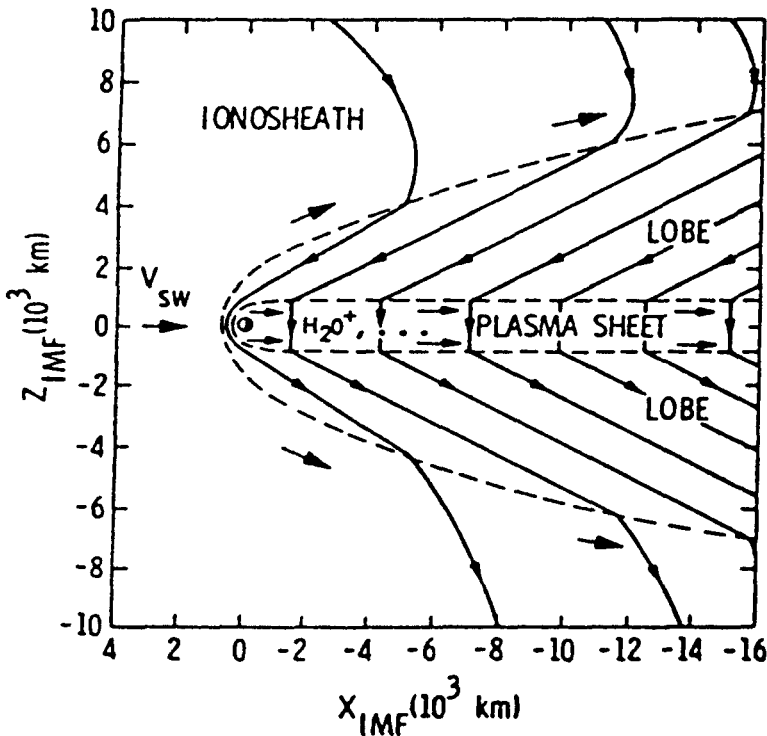

Figure 21. Schematic of the tail of comet Giacobini-Zinner as deduced from ICE plasma and field measurements. From Slavin *et al.* (1986c).

$$p + B^2/2\mu_0 \approx p_{sw} \tag{31}$$

where the thermal plasma pressure p includes contributions from all plasma populations, including cold electrons, superthermal electrons, and hot ions. p_{sw} is the total pressure of the solar wind (in the orthogonal direction and not including dynamic pressure therefore). $p_{sw} \approx n_{sw} k T_{esw}$, where T_{esw} is the electron temperature in the solar wind. Equation (31) is applicable to the extent that the plasma motion is largely in the anti-sunward direction.

In the plasmasheet, the high density of cold plasma is such that plasma pressure makes the dominant contribution to the total pressure, whereas in the tail lobes, the magnetic pressure term is most important. The following relation approximately holds across the plasmasheet boundary (Slavin *et al.*, 1986a,b):

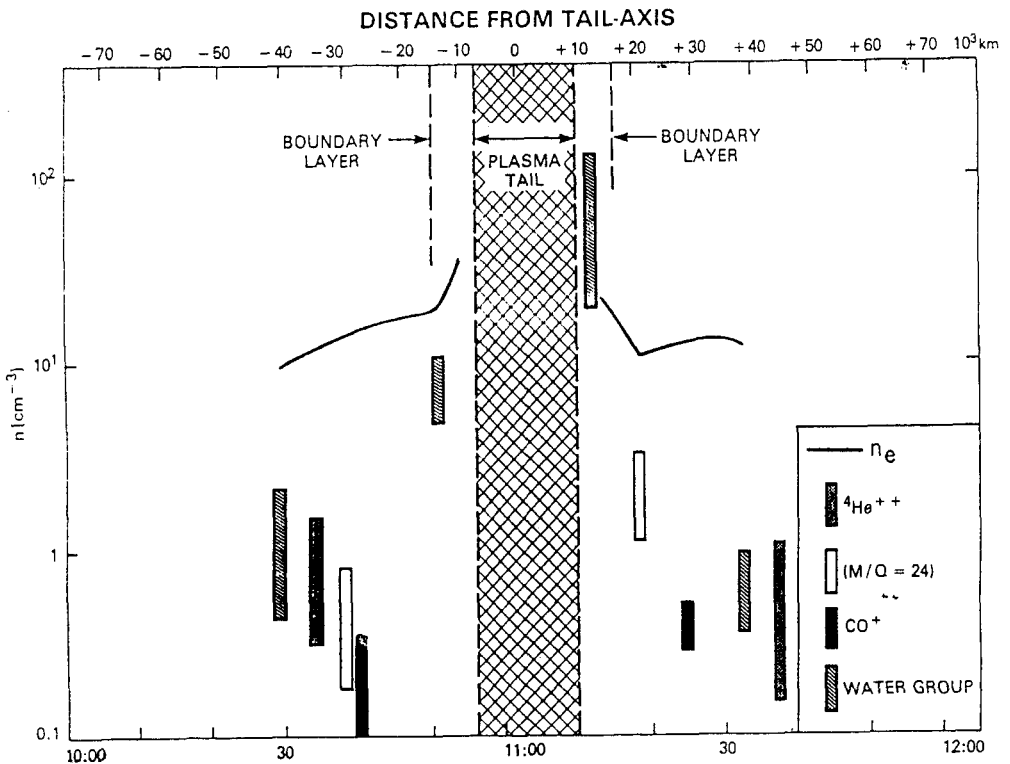$$p_{plasmasheet} = B_{lobe}^2 / 2\mu_0 \tag{32}$$

Figure 22. Number densities of different species of ions measured in the tail of comet Giacobini-Zinner by the Ion Composition Instrument on ICE. From Ogilvie *et al.* (1986).

A similar relation holds at the interface of the magnetosheath with the magnetotail/lobe, although in the magnetosheath (unlike the plasmasheet), the thermal pressure is provided by a very hot, dilute plasma. In fact, many different particle populations mix in the tail region, just as they did in the inner coma, with the more energetic populations originating further upstream. Recall that Zwickl *et al.* (1986) observed several superthermal electron components downstream of G-Z. Very energetic ions (tens of keV) were also observed in the tail region, although their density in the plasmasheet itself was found to be rather low and was attributed to gyroradius effects (Daly *et al.*, 1986). Warm ions were also observed outside the plasmasheet and were identified both as water group ions and CO^+ ions (Ogilvie *et al.*, 1986; Coplan *et al.*, 1987 -- see Figure 22).

The momentum balance relation along the tail axis must include (Siscoe *et al.*, 1986) the dynamic pressure of the plasma flowing down the tail, as well as the axial component of the $J \times B$ force:

$$\rho\, u^2 \;+\; p \;\approx\; \int J \times B\, dx \tag{33}$$

where u is the flow speed down the tail, and the Maxwell stress term is integrated along the tail axis starting from the inner coma where $u \approx 0$. The most important term of $J \times B$ in the neutral sheet is the curvature force, which accelerates the plasma in the anti-solar direction due to the draping pattern of the field lines. The decrease of the density ρ with increasing r also contributes to the acceleration.

8. Summary

The solar wind interaction with comets is characterized by the pick-up of cometary ions that are created by the ionization of cometary neutrals. The solar wind interaction is largely determined by collisionless plasma processes far from the nucleus, other than the initial ionization event. But collisional processes become very important in the inner coma. The following general conclusions about plasma processes in the inner coma can be made:

(1) Several plasma populations exist in the inner coma. The characteristics of a particular population are largely determined by how far upstream the population was created.

(2) All particle populations in the inner coma are strongly affected by collisional processes, such as charge-transfer, ion-neutral chemistry, ion-neutral friction, and thermal cooling.

(3) Plasma processes, in the form of magnetohydrodynamics, are also important in the inner coma.

REFERENCES

Aiken, A. L. (1974). Cometary coma ions, *Astrophys. J.*, **193**, 263.

Allen, M., Delitsky, M., Huntress, W., Yung, Y., Ip, W.-H., Schwenn, R., Rosenbauer, H., Shelley, E., Balsiger, H., and Geiss, J. (1987). Evidence for methane and ammonia in the coma of comet P/Halley, *Astron. Astrophys.*, **187**, 502-512.

Balsiger, H. (1989). Measurements of ion species within the coma of comet Halley from Giotto, in *Comet Halley, World Wide Investigations, Results and Interpretations*, Ellis Horwood Ltd., Chichester, England.

Balsiger, H., Altwegg, K., Bühler, F., Geiss, J., Ghielmetti, A. G., Goldstein, B. E., Goldstein, R., Huntress, W. T., Ip, W.-I., Lazarus, A. J., Meier, A., Neugebauer, M., Rettenmund, U., Rosenbauer, H., Schwenn, R., Sharp, R. D., Shelley, E. G., Ungstrup, E., and Young, D. T. (1986). Ion composition and dynamics at comet Halley, *Nature*, **321**, 330.

Bame, S. J., Anderson, R. C., Asbridge, J. R., Baker, D. N., Feldman, W. C., Fuselier, S. A., Gosling, J. T., McComas, D. J., Thomsen, M. F., Young, D. T., and Zwickl, R. D. (1986). Comet Giacobini-Zinner: Plasma description, *Science*, **232**, 356.

Banks, P. M., and Kockarts, G. (1973). *Aeronomy*, Academic Press, New York.

Baumgartel, K., and Sauer, K. (1987). Fluid simulation of comet P/Halley's ionosphere, *Astron. Astrophys.*, **187**, 307-310.

Biermann, L., Brosowski, P., and Schmidt, H. U. (1967). The interaction of the solar wind with a comet, *Solar Physics*, **1**, 254.

Boice, D. C., Huebner, W. F., Keady, J. J., Schmidt, H. U., and Wegmann, R. (1986). A model of comet P/Giacobini-Zinner, *Geophys. Res. Lett.*, **13**, 381.

Brace, L. H., Theis, R. F., Noegy, W. R., Wolfe, J. H., Mihalov, J. D., Russell, C. T., Elphic, R. C., and Nagy, A. F. (1980). The dynamic behavior of the Venus ionosphere in response to solar wind interactions, *J. Geophys. Res.*, **85**, 7663-7678.

Brandt, J. C. (1982). Observations and dynamics of plasma tails, in *Comets*, ed. L. L. Wilkening, Univ. Arizona, Tucson, p. 519.

Buti, B., and Eviatar, A. (1989). Plasma conductivity for comet Halley's ionosphere, *Astrophys. J.*, **336**, L71.

Coplan, M. A., Ogilvie, K. W., A'Hearn, M. F., Boschler, P., and Geiss, J. (1987). Ion composition and upstream solar wind observations at comet Giacobini-Zinner, preprint.

Cravens, T. E. (1986). The physics of the cometary contact surface, in *Proc. of 20th ESLAB Symposium on the Exploration of Halley's Comet*, eds. B. Battrick, E. J. Rolfe and R. Reinhard, ESA SP-250, **1**, 241.

Cravens, T. E. (1987a). Theory and observations of cometary ionospheres, *Adv. Space Res.*, **7**, 147.

Cravens, T. E. (1987b). Ion energetics in the inner coma of comet Halley, *Geophys. Res. Lett.*, **14**, 983.

Cravens, T. E. (1987c). Test particle calculations of ion distribution of functions near comets, talk presented at IUGG XIX General Assembly (IAGA), Vancouver, August 1987.

Cravens, T. E. (1989a). Cometary plasma boundaries, *Adv. Space Res.*, proc. of 1988 COSPAR meeting, vol. 9, no. 3, pp. 3293-3304, edited by T. I. Gombosi, S. K. Atreya, E. Grün, and M. S. Hanner, Pergamon Press, Oxford.

Cravens, T. E. (1989b). A magnetohydrodynamical model of the inner coma of comet Halley, *J. Geophys. Res.*, **94**, 15025.

Cravens, T. E. (1989c). The solar wind interaction with non-magnetic bodies and the role of small-scale structures, in *Solar System Plasma Physics,* Geophysical Monograph 54, eds. J. H. Waite, Jr., J. L. Burch, and R. L. Moore, p. 353.

Cravens, T. E., and Korosmezey, A. (1986). Vibrational and rotational excitation cooling of electrons by water vapor, *Planet. Space Sci.*, **34**, 961.

Cravens, T. E., Kozyra, J. U., Nagy, A. F., Gombosi, T. I., and Kurtz, M. (1987). Electron impact ionization in the vicinity of comets, *J. Geophys. Res.*, **92**, 7341.

Daly, P. W., Sanderson, T. R., Wenzel, K.-P., Cowley, S. W. H., Hynds, R. J., and Smith, E. J. (1986). Gyroradius effects on the energetic ions in the tail lobes of comet P/Giacobini-Zinner, *Geophys. Res. Lett.*, **13**, 419.

Ershkovich, A. I. (1981). On the magnetic field in the tail of comet Halley, in *The Moon and the Planets*, D. Reidel, Hingham, MA, **25**, p. 521.

Ershkovich, A. I., and Flammer, K. R. (1988). Nonlinear stability of the dayside cometary ionopause, *Astrophys. J.*, **328**, 967.

Ershkovich, A. I., Flammer, K. R., and Mendis, D. A. (1986). Stability of the sunlit cometary ionopause, *Astrophys. J.*, **311**, 1031.

Ershkovich, A. I., McKenzie, J. F., and Axford, W. I. (1989). Stability of a cometary ionosphere/ionopause determined by ion-neutral friction, *Astrophys. J.*, **344**, 932.

Eviatar, A., and Goldstein, B. E. (1989). A unidimensional model of comet ionopause structure, *J. Geophys. Res.*, **93** , 1759.

Eviatar, A., Goldstein, R., Young, D. J., Balsiger, H., Rosenbauer, H., and Fuselier, S. (1989). Energetic ion fluxes in the inner coma of comet Halley, *Astrophys. J.*, **334**, 545.

Fedder, J. A., Lyon, J. G., and Giuliani, J. L., Jr. (1986). Numerical simulations of comets: Predictions for comet Giacobini-Zinner, *Trans. Am. Geophys. Union*, **67**, 17.

Formisano, V., Amata, E., Cattaneo, M. B., Torrente, P., Johnstone, A. D., Coates, A., Wilken, B., Jockers, K., Thomsen, J. F., Winningham, D., and Borg, H. (1988). Plasma flow inside comet P/Halley, submitted to *Astron. Astrophys.*

Fuselier, S. A., Shelley, E. G., Balsiger, H., Geiss, J., Goldstein, B. E., Goldstein, R., and Ip, W.-H. (1988). Cometary H_2^+ and solar wind He^{++} dynamics across the Halley cometopause, *Geophys. Res. Lett.*, **15**, 549.

Galeev, A. A. (1986). Theory and observations of solar wind/cometary plasma interaction processes, in *Proc. of 20th ESLAB Symposium on the Exploration of Halley's Comet*, eds. B. Battrick, E. J. Rolfe and R. Reinhard, ESA SP-250, **1**, 3.

Galeev, A. A. (1990). This book.

Galeev, A. A. and Lipatov, A. S. (1984). Plasma processes in cometary atmospheres, *Adv. Space Res.*, **4**, 229.

Galeev, A. A., Cravens, T. E., and Gombosi, T. I. (1985). Solar wind stagnation near comets, *Astrophys. J.*, **289**, 807.

Galeev, A. A., Gringauz, K. I., Klimov, S. I., Remizov, A. P., Sagdeev, R. Z., Savin, S. P., Sokolov, A. Yu., Verigin, M. I., and Szego, K. (1986). Critical ionization velocity effects in the inner coma of comet Halley: Measurements by VEGA-2, *Geophys. Res. Lett.*, **13**, 845.

Galeev, A. A., Gringauz, K. I., Klimov, S. I., Remizov, A. P., Sagdeev, R. Z., Savin, S. P., Sokolov, A.Yu., Verigin, M. I., Szego, K., Tatrallyay, M., Grard, R., Yeroshenko, Ye. G., Mogilevsky, M., Riedler, W., Schwingenschuh, K. (1988). Physical processes in the vicinity of the cometopause interpreted on the basis of plasma, magnetic field, and plasma wave data measured on board the VEGA 2 spacecraft, *J. Geophys. Res.*, **93**, 7527.

Gan, Lu, and Cravens, T. E. (1990). Electron energetics in the inner coma of comet Halley, *J. Geophys. Res.*, in press.

Goldstein, R., Young, D. T., Balsiger, H., Buhler, F., Goldstein, B. E., Neugebauer, M., Rosenbauer, H., Schwenn, R., and Shelley, E. G. (1987). Hot ions observed by the Giotto ion mass spectrometer at the comet P/Halley contact surface, *Astron. Astrophys.*, **187**, 20.

Goldstein, B. E., Schwenn, R., Ip, W.-H, Balsiger, H., Meier, A., Altwegg, K., Rosenbauer, H., Neugebauer, M., and Fuselier, S. A. (1989). Observations of a shock and recombination layer at the contact surface of comet Halley, *J. Geophys. Res.*, **94**, 17251.

Gombosi, T. I. (1987). Charge exchange avalanche at the cometopause, *Geophys. Res. Lett.*, **14**, 1174.

Gombosi, T. I., Nagy, A. F., and Cravens, T. E. (1986). Dust and neutral gas modeling of the inner atmospheres of comets, *Rev. Geophys.*, **24**, 667.

Grard, F., Scarf, F., Trotignon, J. G., and Mogilevsky, M. (1987). A comparison between wave observations performed in the environments of comets Halley and Giacobini-Zinner, in *Proc. of the Symposium on the Diversity and Similarity of Comets*, 6-7 April 1987, Brussels, Belgium, ESA SP-278, p. 97.

Gringauz, K. I., Gombosi, T. I., Remizov, A. P., Apáthy, I., Szemerey, I., Verigin, M. I., Denchikova, L. I., Dyachkov, A. V., Keppler, E., Klimenko, I. N., Richter, A. K., Somogyi, A. J., Szegö, K., Szendrö, S., Tátrallyay, M., Varga, A., and Vladimirova, G. A. (1986a). First in situ plasma and neutral gas measurements at comet Halley, *Nature*, **321**, 282.

Gringauz, K. I., Gombosi, T. I., Tatrallyay, M., Verigin, M. I., Remizov, A. P., Richter, A. K., Apathy, I., Szemerey, I., Pyachkov, A. V., Balakina, O. V., and Nagy, A. F. (1986b). Detection of a new "chemical" boundary at comet Halley, *Geophys. Res. Lett.*, **13**, 613.

Haerendel, G. (1986). Plasma flow and critical velocity ionization in cometary comae, *Geophys. Res. Lett.*, **13**, 255.

Haerendel, G. (1987). Plasma transport near the magnetic cavity surrounding comet Halley, *Geophys. Res. Lett.*, **14**, 673.

Houpis, H. L. F. (1988). The global interaction of comets with the solar wind: Heliocentric variation, in *Symposium on Physical Interpretations of Solar/Interplanetary and Cometary Intervals*, ed. M. A. Shea.

Houpis, H. L. F., and Mendis, D. A. (1980). Physiochemical and dynamical processes in cometary ionospheres 1. The basic flow profile, *Astrophys. J.*, **239**, 1107.

Huebner, W. F. (1985). The photochemistry of comets, in *The Photochemistry of Atmospheres*, Academic Press, p. 437.

Huebner, W. F. (1990). This book.

Huntress, W. T., Ip, W.-H., Lazarus, A. J., Meier, A., Neugebauer, M., Rettenmudd, U., Rosenbauer, H., Schwenn, R., Sharp, R. D., Shelley, E. G., Ungstrup, E., and Young, D.T. (1986). Ion composition and dynamics at comet Halley, *Nature*, **321**, 330.

Ip, W.-I. (1989). On the charge exchange effect in the vicinity of the cometopause of comet Halley, *Astrophys J.*, **343**, 946.

Ip, W.-H. and Axford, W. I. (1982). Theories of physical processes in the cometary comae and ion tails, in *Comets*, ed. L.L. Wilkening, University of Arizona Press, Tucson, p. 588.

Ip, W.-H., and Axford, W. I. (1987). The formation of a magnetic field free cavity at comet Halley, *Nature*, **325**, 418.

Ip, W.-H., and Axford, W. I. (1989). Cometary plasma physics, to appear in *Physics of Comets in the Space Age*, ed. W. F. Huebner.

Ip, W.-H., Schwenn, R., Rosenbauer, H., Balsiger, H., Neugebauer, M., and Shelley, E. G. (1987). An interpretation of the ion pile-up region outside the ionospheric contact surface, *Astron. Astrophys.*, **187**, 132-136.

Ip, W.-H., Cosmovici, C. B., and Mack, P. (1986). A comparison of ground-based CCD H_2O^+ observations with the Giotto measurements at comet Halley, in *Proc. of 20th ESLAB Symposium on the Exploration of Halley's Comet*, eds. B. Battrick, E. J. JRolfe, and R. Reinhard, ESA SP-250, **1**, 507.

Johnstone, A., Coates, A., Kellock, S., Wilken, B., Jockers, K., Rosenbauer, H., Studemann, W., Weiss, W., Formisano, V., Amata, E., Cerulli-Irelli, R., Dobrowolny, M., Terenzi, R., Egidi, A., Borg, H., Hultqvist, B., Winningham, J., Gurgiolo, C., Bryant, D., Edwards, T., Feldman, W., Thomsen, M., Wallis, M. K., Biermann, L., Schmidt, H., Lust, R., Haerendel, G., and Paschmann, G. (1986). Ion flow at comet Halley, *Nature*, **321**, 344.

Kirsch, E., McKenna-Lawlor, S., O'Sullivan, D., Thompson, A., and Daly, P. W. (1987). Observation of energetic particles (E>30 keV) by the Giotto experiment EPA in the magnetic cavity of comet Halley, in *Proceedings of the Symposium on the Diversity and Similarity of Comets*, 6-9 April, 1987, Brussels, Belgium, ESA SP-278, 145.

Konno, I. (1989). An emission profile of H_2O^+ for comet P/Giacobini-Zinner at the time of the ICE encounter, *Astron. Astrophys.*, submitted.

Körösmezey, A., Cravens, T. E., Gombosi, T. I., Nagy, A. F., Mendis, D. A., Szegö, K., Gribov, B. E., Sagdeev, R. Z., Shapiro, V. D., and Shevchenko, V. I. (1987). A comprehensive model of cometary ionospheres, *J. Geophys. Res.*, **92**, 7331.

Krankowsky, D., Lämmerzahl, P., Herrwerth, L., Woweries, J., Eberhardt, P., Dolder, U., Hermann, U., Schulte, W., Berthelier, J. J., Illiano, J. M., Hodges, R. R., and Hoffman, J. H. (1986). In situ gas and ion measurements at comet Halley, *Nature*, **321**, 326.

Lee, M. C. (1989). Ultra-low frequency waves at comets, in *Plasma Waves and Instabilities at Comets and in Magnetospheres*, Geophysical Monograph 53, eds. B. Tsurutani and H. Oya, p. 239.

Marconi, M. L., and Mendis, D. A. (1986). The electron density and temperature in the tail of comet Giacobini-Zinner, *Geophys. Res. Lett.*, **13**, 405.

Marconi, M. L., and Mendis, D. A. (1988). On the ammonia abundance in the coma of Halley's Comet, *Astrophys. J.*, **330**, 513.

McKenna-Lawlor, S., Kirsch, E., O'Sullivan, D., Thompson, A., and Wenzel, K.-P. (1986). Energetic ions in the environment of comet Halley, *Nature*, **321**, 347.

Mendis, D. A., and Houpis, H. L. F. (1982). The cometary atmosphere and its interaction with the solar wind, *Rev. Geophys. Res.*, **20**, 885.

Mendis, D. A., Houpis, H. L. F., and Marconi, M. L. (1985). The physics of comets, *Fund. Cosmic Phys.*, **10**, 1.

Meyer-Vernet, N., Couturier, P., Hoang, S., Perche, C., Steinberg, J. L., Fainberg, J., and Meetre, C. (1986). Plasma diagnosis from thermal noise and limits on dust flux or mass in comet P/Giacobini-Zinner, *Science*, **232**, 370.

Mogilevsky, M., Mikhailov, Y., Molchanov, O., Grard, R., Pedersen, A., Trotignon, J. G., Beghin, C., Formisano, V., Shapiro, V., and Shevchenko, V. (1987). Identification of boundaries in the cometary environment from AC electric field measurements, *Astron. Astrophys.*, **187**, 80-82.

Mukai, T., Miyake, W., Terasawa, T., Kitayama, M. and Kirao, K. (1986a). Plasma observation by Suisei of solar wind interaction with comet Halley, *Nature*, **321**, 299.

Mukai, T., Miyake, W., Terasawa, T., Kitayama, M., and Kirao, K. (1986b). Ion dynamics and distribution around comet Halley: Suisei observation, *Geophys. Res. Lett.*, **13**, 829.

Neubauer, F. M. (1986). Giotto magnetic field results on the magnetic field pile-up region and the cavity boundaries, in *Proc. of 20th ESLAB Symposium on the Exploration of Halley's Comet*, eds. B. Battrick, E. J. Rolfe and R. Reinhard, ESA SP-250, **1**, 35.

Neubauer, F. M. (1987). Giotto magnetic field results on the boundaries of the pile-up region and the magnetic cavity, *Astron. Astrophys.*, **187**, 73.

Neubauer, F. M. (1988). The ionopause transition and boundary layers at comet Halley from Giotto magnetic field observations, *J. Geophys. Res.*, **93**, 1282.

Neubauer, F. M. (1990). This book.

Neubauer, F. M., Glassmeier, K. H., Pohl, M., Raeder, J., Acuna, M. H., Burlaga, L. F., Ness, N. F., Musmann, G., Mariani, F., Wallis, M. K., Ungstrup, E., and Schmidt, H. U. (1986). First results from the Giotto magnetometer experiment at comet Halley, *Nature,* **321**, 352.

Neugebauer, M., Neubauer, F. M., Balsiger, H., Fuselier, S. A., Goldstein, B. E., Goldstein, R., Mariani, F., Rosenbauer, H., Schwenn, R., and Shelley, E. G. (1987). The variation of protons, alpha particles, and the magnetic field across the bow shock of comet Halley, *Geophys. Res. Lett.*, **14**, 995.

Neugebauer, M. (1990). Spacecraft observations of the interaction of active comets with the solar wind, *Reviews of Geophysics*, vol. 28, in press.

Ogilvie, K. W., Coplan, M. A., Boschler, P., and Geiss, J. (1986). Ion composition results during the International Cometary Explorer encounter with Giacobini-Zinner, *Science*, **232**, 374.

Ogino, T., Walker, R. J., and Ashour-Abdalla, M. (1988). A three-dimensional MHD simulation of the interaction of the solar wind with comet Halley, *J. Geophys. Res.*, **93**, 9568.

Omidi, N., Winski, D., and Wu, C. S. (1986). The effect of heavy ions on the formation and structure of cometary bow shocks, *Icarus*, **66**, 165.

Reme, H., Sauvaud, J. A., D'Uston, C., Cotin, F., Cros, A., Anderson, K. A., Carlson, C. W., Curtis, D. W., Lin, R. P., Mendis, D. A., Korth, A., and Richter, A. K. (1986). Comet Halley--Solar wind interaction from electron measurements aboard Giotto, *Nature*, **321**, 349.

Riedler, W., Schwingenschuh, K., Yeroshenko, Ye. G., Styashkin, V. A., and Russell, C. T. (1986). Magnetic field observations in comet Halley's coma, *Nature*, **321**, 288.

Russell, C. T. (1988). The interaction of the solar wind with comet Halley: Upwind and downwind, *Q. J. R. Astr. Soc.*, **29**, 157.

Russell, C. T., Riedler, W., Schwingenschuh, K., and Yeroshenko, Ye. (1987). Mirror instability in the magnetosphere of comet Halley, *Geophys. Res. Lett.,* **14**, 644.

Sauer, K. and Baumgärtel, K. (1986). Fluid simulation of Halley's ionosphere, in *Proc. of 20th ESLAB Symposium on the Exploration of Halley's Comet,* eds. B. Battrick, E. J. Rolfe and R. Reinhard, ESA SP-250, **3**, 401.

Sauer, K., Motschmann, U., and Roatsch, J. (1989). Plasma boundaries at comet Halley, *Annales Geophysicae*, in press.

Schmidt, H. U., and Wegmann, R. (1982). Plasma flow and magnetic fields in comets, in *Comets*, ed. L.L. Wilkening, Univ. Arizona, Tucson, p. 538.

Schmidt, H. U., Wegmann, R., and Neubauer, F. M. (1986). MHD model for comet Halley, in *Proc. of 20th ESLAB Symposium on the Exploration of Halley's Comet*, eds. B. Battrick, E. J. Rolfe and R. Reinhard, ESA SP-250, **1**, 43.

Schmidt, H. U., Wegmann, R., Huebner, W. F., and Boice, D. C. (1988). Cometary gas and plasma flow with detailed chemistry, *Computer Phys. Comm.*, **49**, 17.

Schmidt-Voigt, M. (1989). Time dependent MHD simulations for cometary plasmas, *Astron. Astrophys.*, **210**, 433.

Schwenn, R., Ip, W.-H., Rosenbauer, H., Balsiger, H., Buhler, F., Goldstein, R., Meier, A., and Shelley, E. G. (1986). Ion temperature and flow profiles in comet Halley's close environment, in *Proc. of 20th ESLAB Symposium on the Exploration of Halley's Comet*, eds. B. Battrick, E. J. Rolfe and R. Reinhard, ESA SP-250, **1**, 225.

Schwenn, R., Ip, W.-H., Rosenbauer, H., Balsiger, H., Buhler, F., Goldstein, R., Meier, A., and Shelley, E. G. (1987). Ion temperature and flow profiles in comet P/Halley's close environment, *Astron. Astrophys.*, **187**, 160-162.

Schwingenschuh, K., Riedler, W., Yeroshenko, Ye., Phillips, J. L., Russell, C. T., Luhmann, J. G., and Fedder, J. A. (1987). Magnetic field draping in the comet Halley coma: Comparison of VEGA observations with computer simulations, *Geophys. Res. Lett.*, **14**, 640.

Shelley, E. G., Fuselier, S. A., Balsiger, H., Drake, J. F., Geiss, J., Goldstein, B. E., Goldstein, R., Ip, W.-I., Lazarus, A. J., and Neugebauer, M. (1987). Charge exchange of solar wind ions in the coma of comet P/Halley, *Astron. Astrophys.*, **187**, 304-306.

Siscoe, G. L. (1983). Solar system magnetohydrodynamics, in *Solar Terrestrial Physics*, eds. R.L. Carovillano and J.M. Forbes, D. Reidel Co., Dordrecht, p. 11.

Siscoe, G. L., Slavin, J. A., Smith, E. J., Tsurutani, B. T., Jones, D. E., and Mendis, D. A. (1986). Statics and dynamics of Giacobini-Zinner magnetic tail, *Geophys. Res. Lett.*, **13**, 287.

Slavin, J. A., Smith, E. J., Tsurutani, B. T., Siscoe, G. L., Jones, D. E., and Mendis, D. A. (1986a). Giacobini-Zinner magnetotail: ICE magnetic field observations, *Geophys. Res. Lett.*, **13**, 283.

Slavin, J. A., Goldberg, B. A., Smith, E. J., McComas, D. J., Bame, S. J., Strauss, M. A., and Spinrad, H. (1986b). The structure of a cometary type 1 tail: Ground-based and ICE observations of P/Giacobini-Zinner, *Geophys. Res. Lett.*, **13**, 1085-1088.

Slavin, J. A., Smith, E. J., Daly, P. W., Flammer, K. R., Gloeckler, G., Goldberg, B. A., McComas, D. J., Scarf, F. L., and Steinberg, J. L. (1986c). The P/Giacobini-Zinner magnetotail, in *Proc. of 20th ESLAB Symposium on the Exploration of Halley's Comet*, eds. B. Battrick, E. J. Rolfe and R. Reinhard, ESA SP-250, **1**, 81-87.

Somogyi, A. J., Gringauz, K. I., Szegö, K., Szabó, L., Kozma, Gy., Remizov, A. P., Erö, J., Jr., Klimenko, I. N., Szücs, I. T., Verigin, M. I ., Windberg, J., Cravens, T. E., Dyachkov, A., Erdös, G., Faragó, M., Gombosi, T. I., Kecskeméty, K., Keppler, E., Kovács, T., Jr., Kondor, A., Logachev, Uy. I., Lohonyai, L., Marsden, R., Redl, R., Richter, A. K., Stolpovskii, V. G., Szabó, J., Szentpétery, I., Szepesváry, A., Tátrallyay, M., Varga, A., Vladimirova, G. A., Wenzel, K.-P., and Zarándy, A. (1986). First observations of energetic particles near comet Halley, *Nature*, **321**, 285.

Spenner, K., Knudsen, W. C., Miller, K. L., Novak, V., Russell, C. T., and Elphic, R. C. (1980). Observation of the Venus mantle: The boundary region between solar wind and ionosphere, *J. Geophys. Res.*, **85**, 7655.

Terasawa, J. (1989). Particle scattering and acceleration in a turbulent plasma around comets, in *Plasma Waves and Instabilities at Comets and in Magnetospheres*, Geophysical Monograph 53, eds. B. Tsurutani and H. Oya, p. 239.

Tsurutani, B. (1990). This book.

Verigin, M. I., Gringauz, K. I., Richter, A. K., Gombosi, T. I., Remizov, A. P., Szego, K., Apathy, I., Szemerey, I., Tatrallyay, M., and Lezhen, L. A. (1987). Plasma properties from the upstream region to the cometopause of comet P/Halley: Vega observations, *Astron. Astrophys.*, **187**, 121-124.

Wallis, M. K., and Dryer, M. (1976). Sun and comets as sources in an external flow, *Astrophys. J.*, **205**, 895.

Wallis, M. K., and Ong, R. S. B. (1974). Cooling and recombination processes in cometary plasmas, in *The Study of Comets*, eds. B. Donn, M. Mumma, W. Jackson, M. A'Hearn, and R. Harrington, NASA SP-393, Washington, D.C., p. 856.

Wallis, M. K., and Ong, R. S. B. (1975). Strongly cooled ionizing plasma flows with application to beams, *Planet. Space Sci.*, **23**, 713.

Wegmann, R., Schmidt, H. U., Huebner, W. F., and Boice, D. C. (1987). Cometary MHD and chemistry, *Astron. Astrophys.*, **187**, 339-350.

Wu, Z.-J. (1987). Calculation of the shape of the contact surface at comet Halley, in *Proceedings of the Symposium on the Diversity and Similarity of Comets*, 6-9 April, 1987, Brussels, Belgium, ESA SP-278.

Zwickl, R. D., Baker, D. N., Bame, S. J., Feldman, W. C., Fuselier, S. A., Huebner, W. F., McComas, D. J., and Young, D. T. (1986). Three component plasma electron distribution in the intermediate ionized coma of comet Giacobini-Zinner, *Geophys. Res. Lett.*, **13**, 401.